
High-Fidelity, Time-Efficient Modeling of Articulated, Flexible Multibody Spacecraft

Arun Banerjee

*Formerly Principal Research Scientist,
Lockheed Martin Advanced Technology Center, Palo Alto*

Examples of Flexible Multibody Spacecraft in Large Overall Motion: Configuration Change, Spin, Slewing, and Antenna “Extrusion”

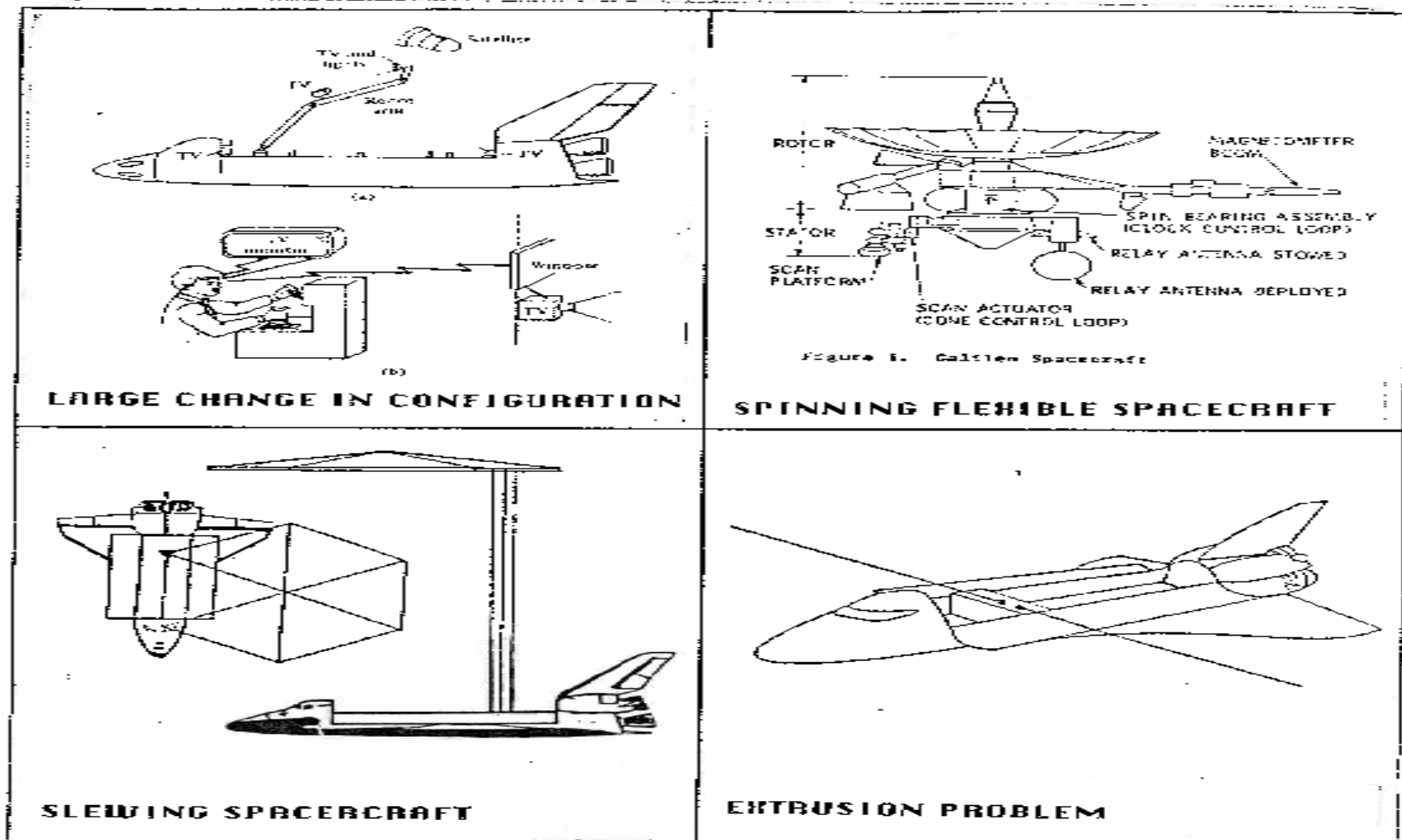


Fig.10 Representative Systems Undergoing Stationkeeping, Constant Spin, Slewing, and Spin-up Motions

JPL's Galileo Spacecraft : A Flexible Multibody System

1. HG flexible antenna rotates w.r.t. flexible stator
 2. RTG booms swivel w.r.t. HG antenna about rotary hinges to provide wobble damping
 3. Scan platform rotates w.r.t. stator in 2 dof hinges
-

Essence: a typical spacecraft is made of several flexible bodies, connected by rotational joints, with the bodies undergoing large rotation with small elastic vibration

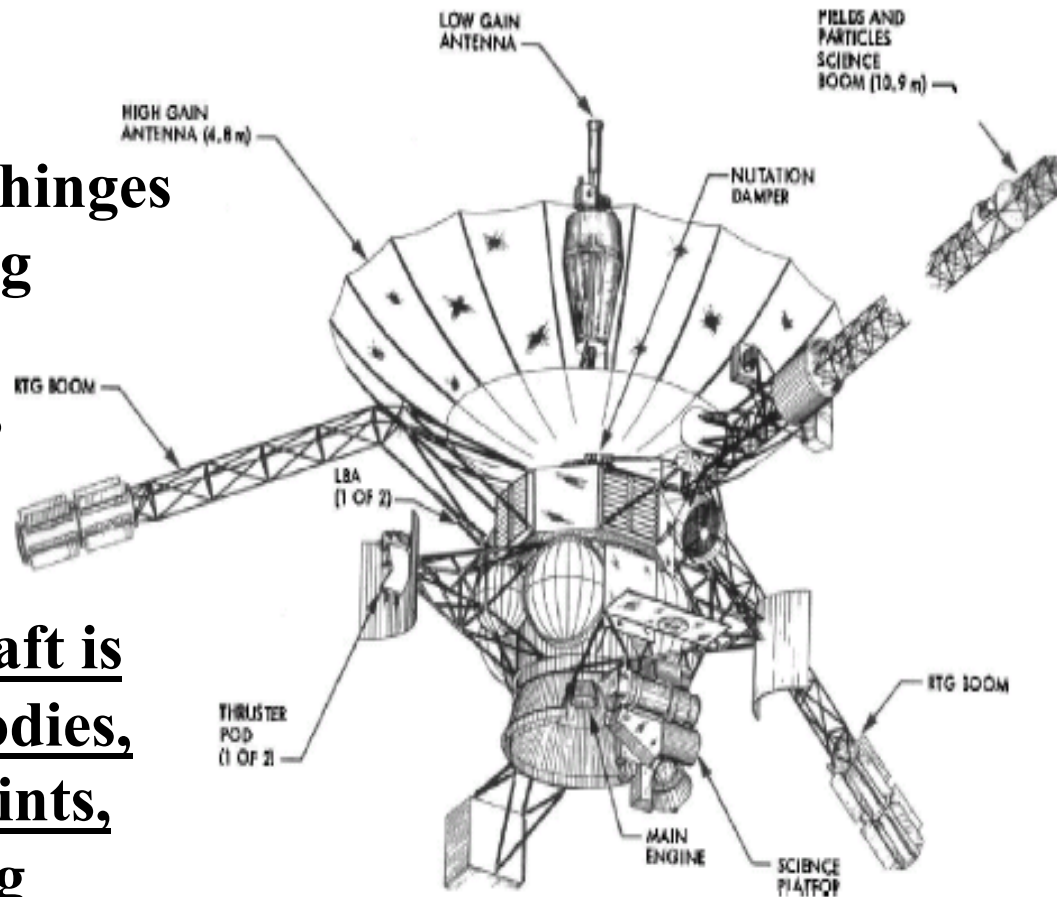


Fig. 1 Galileo spacecraft built by the Jet Propulsion Laboratory.

Studied Jupiter's Atmosphere

Kane's Method of Deriving the Simplest Eqns of Motion by the Least Labor: Example--50 DOF System of 4 Flex Bodies with Rotary Joints

Kane, T. R. and Levinson, D. A., "Formulation of Equations of Motion for Complex Spacecraft," Jour. of Guidance and Control, Mar-Apr 1980, pp. 99-112.

Simplifying motion variables $u_j = \sum_{k=1}^n A_{jk} \dot{q}_k + D_j, \Rightarrow \dot{q}_k = \sum_{j=1}^n W_{kj} u_j + X_k \quad j = 1, \dots, n$

$$\mathbf{v}^k = \sum_{j=1}^n \frac{\partial \mathbf{P}^k}{\partial \dot{q}_j} \dot{q}_j + \frac{\partial \mathbf{P}^k}{\partial t} = \sum_{j=1}^n \frac{\partial \mathbf{v}^k}{\partial u_j} u_j + \mathbf{B}^k$$

Velocity is in terms of j -th Partial Velocities, $\frac{\partial \mathbf{v}^k}{\partial u_j}$
which are functions of gen. coords, q 's

$$\mathbf{a}^k = \sum_{j=1}^n \frac{\partial \mathbf{v}^k}{\partial u_j} \dot{u}_j + \mathbf{C}^k$$

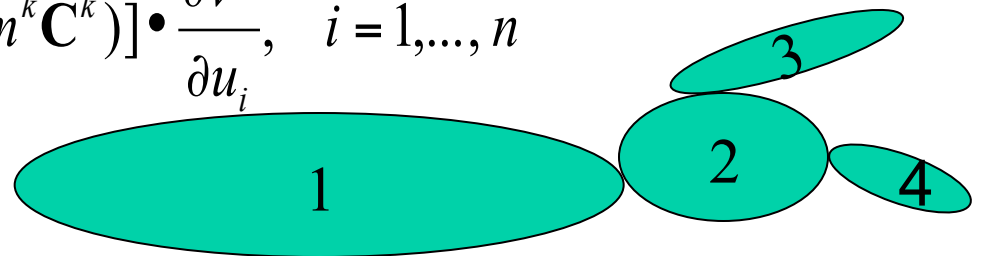
Acceleration of generic point k

$$0 = \sum_{k=1}^{NP} [\mathbf{F}^k + (-m^k \mathbf{a}^k)] \cdot \frac{\partial \mathbf{v}^k}{\partial u_i}, \quad i = 1, \dots, n$$

Use of dot-products make Kane's Equations of least labor

$$\sum_{k=1}^{NP} m^k \sum_{j=1}^n \left[\frac{\partial \mathbf{v}^k}{\partial u_i} \cdot \frac{\partial \mathbf{v}^k}{\partial u_j} \right] \dot{u}_j = \sum_{k=1}^{NP} [\mathbf{F}^k + (-m^k \mathbf{C}^k)] \cdot \frac{\partial \mathbf{v}^k}{\partial u_i}, \quad i = 1, \dots, n$$

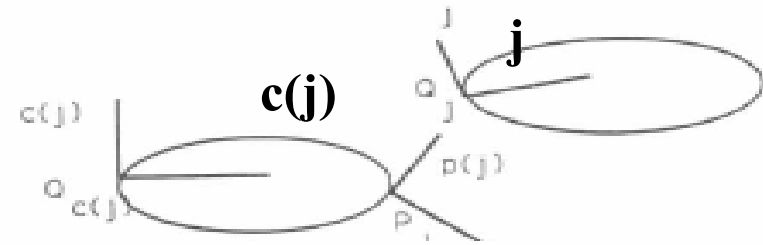
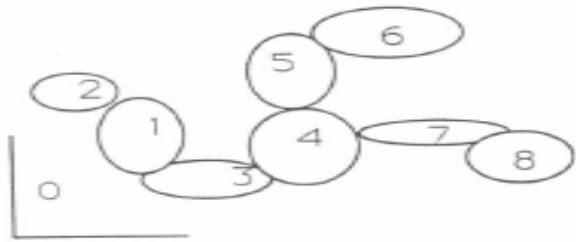
$$[M(q)]\{\dot{U}\} = \{R\}$$



For 50 dof system, form, decompose & solve 50x50 dense, time-varying matrix 4 times per RK step; Unmodified this approach is expensive !

3-Step Recursion of Kane's Eqs for Block-diagonal Matrix Eqs*

Step 1) Form Kinematics Eqns going Forward from Body 1 to Body n



ang. vel. j-frame

$$\omega^j = C_{c(j),j}^T \left[\omega^{c(j)} + \phi^{c(j)}(P_j) \dot{\eta}^{c(j)} + C_{c(j),p(j)} G^j \dot{\theta}^j \right]$$

inboard body ang vel, modal slope rates, gimbal rotation rates

velocity of Qj

$$\begin{aligned} v^{Qj} = & C_{c(j),j}^T \left\{ v^{Qc(j)} + \tilde{\omega}^{c(j)} \left[r^{Qc(j)P_j} + \phi^{c(j)}(P_j) \eta^{c(j)} \right] \right. \\ & + \phi^{c(j)}(P_j) \dot{\eta}^{c(j)} + C_{c(j),p(j)} L^j \dot{\tau}^j + \left[\tilde{\omega}^{c(j)} \right. \\ & \left. \left. + \overline{\phi^{c(j)}(P_j) \dot{\eta}^{c(j)}} \right] C_{c(j),p(j)} L^j \tau^j \right\} \end{aligned}$$

inboard body hinge Pj-velocity, plus account for sliding joint

*Banerjee, A. K., "Block-Diagonal Equations for Flexible Multibody Dynamics with Geometric Stiffness and Constraints", JGCD, Nov. - Dec., 1993, pp. 1092-1100.

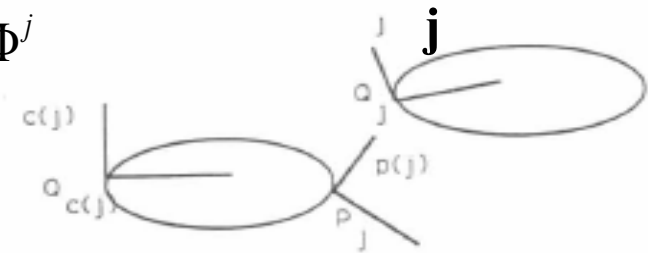
Block-Diagonal Eqns (continued)

Step 2) Form Dynamical Eqns for Body n Going Backward to body1

Write Eqs. for Body j Vibration for Base Accl: invert nmodes x nmodes matrix

$$E^j \ddot{\eta}^j = A^j \begin{Bmatrix} a_0^{Qj} \\ \alpha_0^j \end{Bmatrix} + Y_1^j$$

$$E^j = \Phi^{j^t} M^j \Phi^j$$



$$\begin{Bmatrix} a_0^{Qj} \\ \alpha_0^j \end{Bmatrix} = \begin{Bmatrix} \hat{a}_0^{Qj} \\ \hat{\alpha}_0^j \end{Bmatrix} + R^j \begin{Bmatrix} \ddot{\tau}^j \\ \ddot{\theta}^j \end{Bmatrix}$$

Write Rotn / Tran Newton-Euler Eqs for body j hinge: invert matrix of size 1 to 6

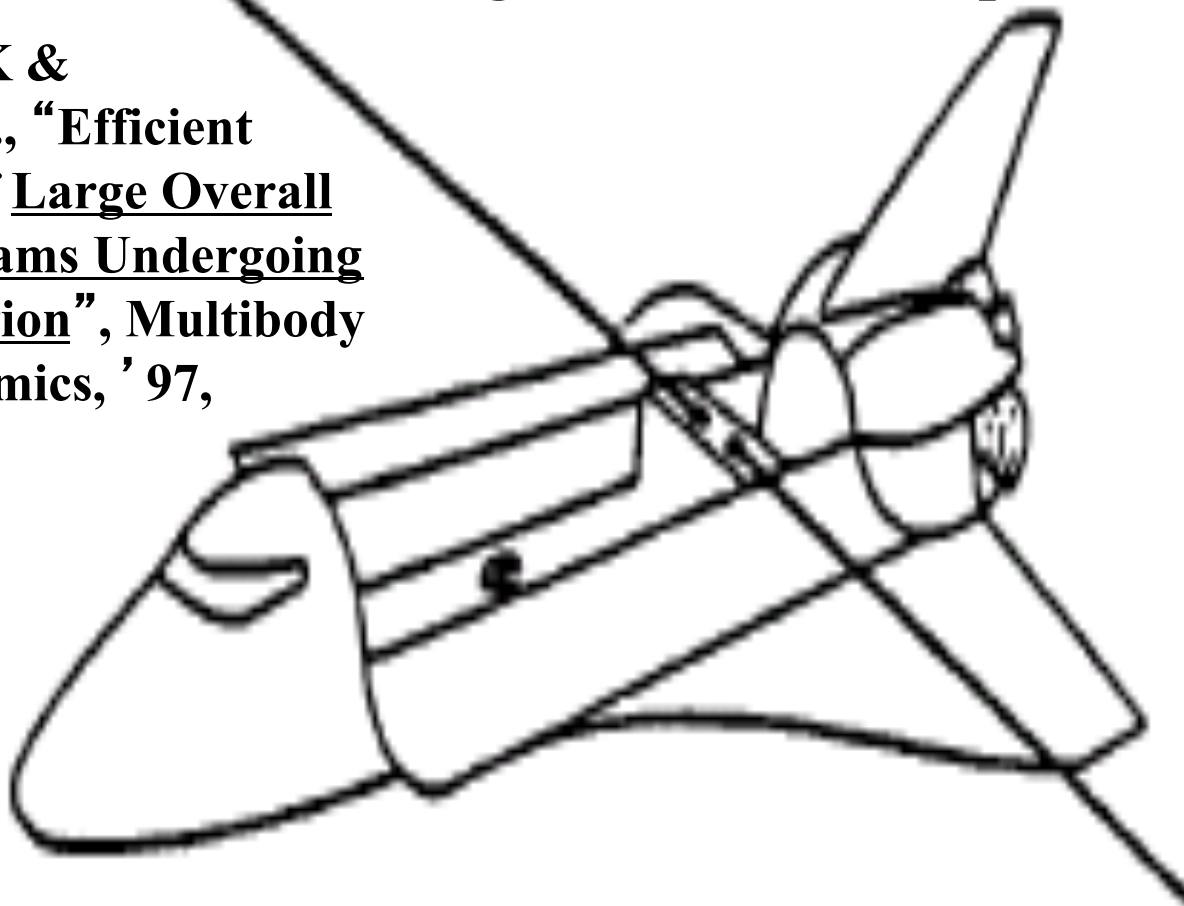
$$\begin{Bmatrix} \ddot{\tau}^j \\ \ddot{\theta}^j \end{Bmatrix} = -\nu^{j-1} R^{j^T} \left[M_3^j \begin{Bmatrix} \hat{a}_0^{Qj} \\ \hat{\alpha}_0^j \end{Bmatrix} + Y_2^j \right] + \nu^{j-1} \begin{pmatrix} f_h^j \\ t_h^j \end{pmatrix} \quad \nu^j = R^{j^t} m^j R^j$$

Step 3) After eqns for body #1 are formed, go forward one more time to explicitly “uncover” eqns for bodies 2,...,n one at a time

Applications: Degenerate Case of Systems of Rigid Bodies

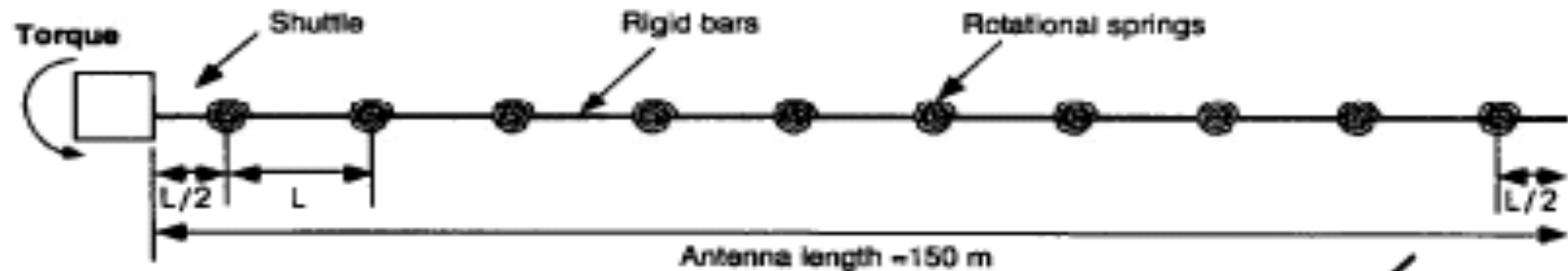
**Two Antenna Booms, each 150 m long, for
Yawing Shuttle WISP experiment**

**Banerjee, A.K &
Nagarajan, S., “Efficient
Simulation of Large Overall
Motion of Beams Undergoing
Large Deflection”, Multibody
System Dynamics, '97,
pp.113-126.**



Shuttle Waves in Space Plasma (WISP) Experiment

Elastic Beam Modeled as Many Rigid Rods Pin-Connected by Rotational Springs, for Large Bending Simulation of 150 m Antenna



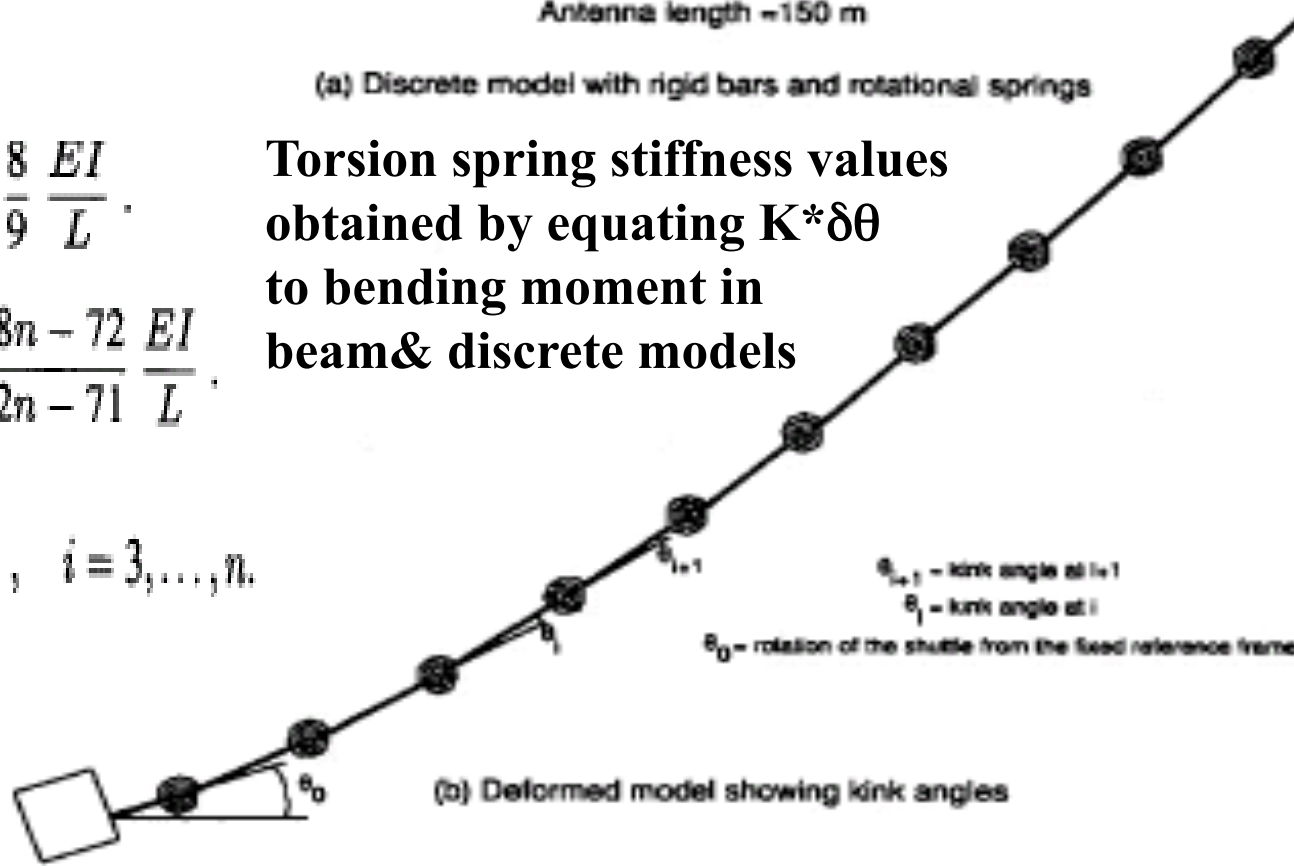
(a) Discrete model with rigid bars and rotational springs

$$\sigma_1 = \frac{8}{9} \frac{EI}{L}$$

$$\sigma_2 = \frac{48n - 72}{42n - 71} \frac{EI}{L}$$

$$\sigma_i = \frac{EI}{L}, \quad i = 3, \dots, n.$$

Torsion spring stiffness values obtained by equating $K \cdot \delta\theta$ to bending moment in beam & discrete models



(b) Deformed model showing kink angles

Rigid Body Order-n vs. Nonlinear FEM for Shuttle WISP Antenna: Large Yaw Angle, Root Bending Moment, Tip Deflection, CPU sec

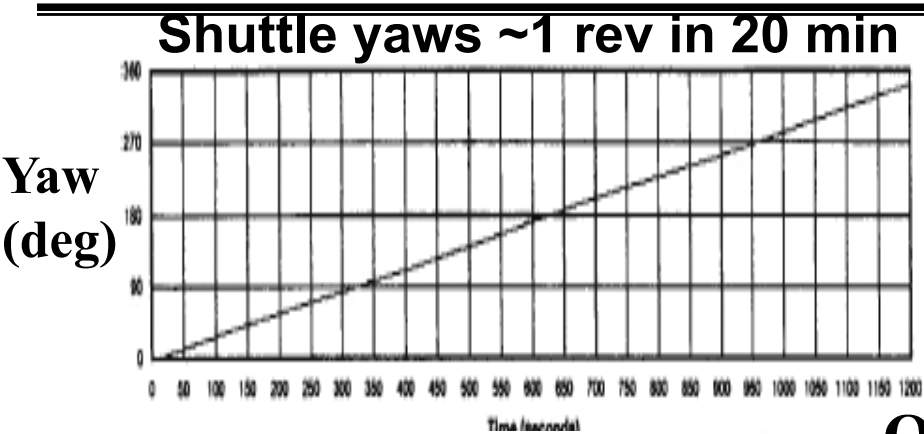


Table I.

Formulation	Number of elements	Step size (sec)	CPU time (sec)
CPU order-n	10	1.0	24
sec order-n	10	0.5	40.9
finite element	10	1.0	890

O(n) Model 36 times faster than FEM

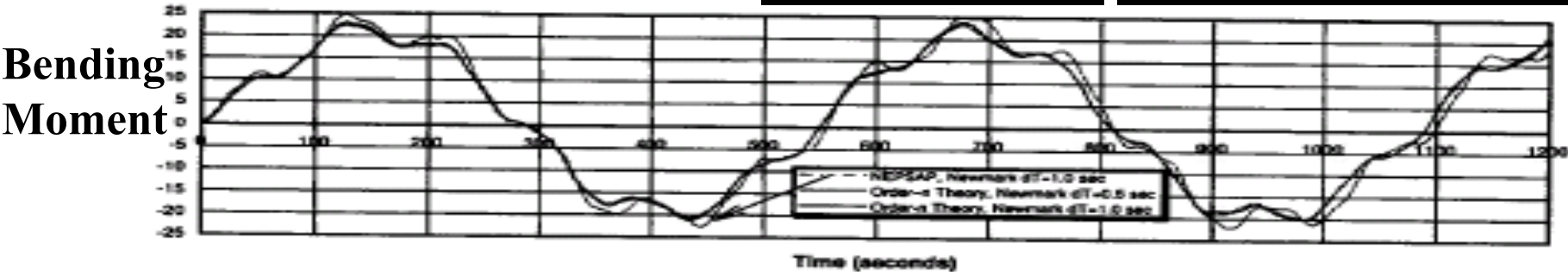
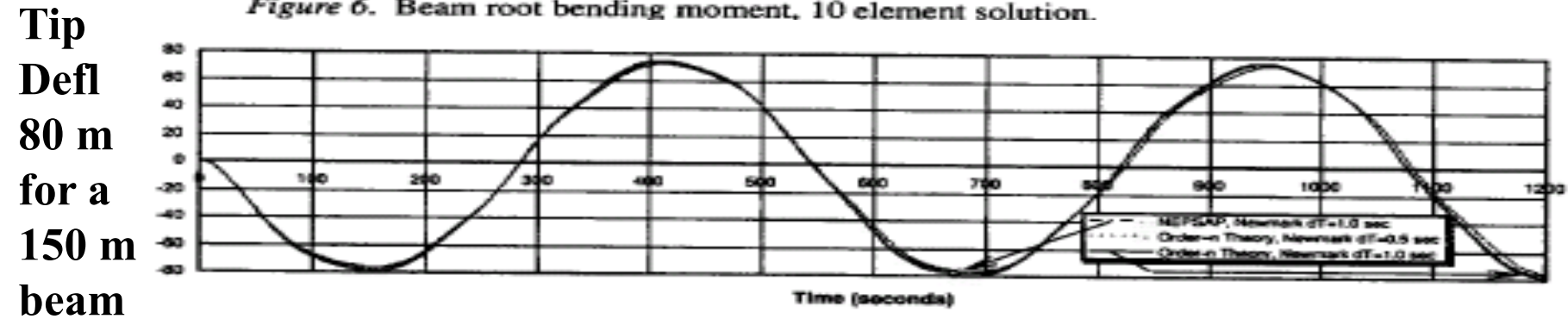


Figure 6. Beam root bending moment, 10 element solution.



Deployment & Retraction Problems : Variable-n O(n) Formulation of two 150 m Booms from Yawing Shuttle [Banerjee, JGCD,1992]

Deployment (telescoping)

Retraction (spaghetti-eating)

Tip
Deflec
max 16 ft

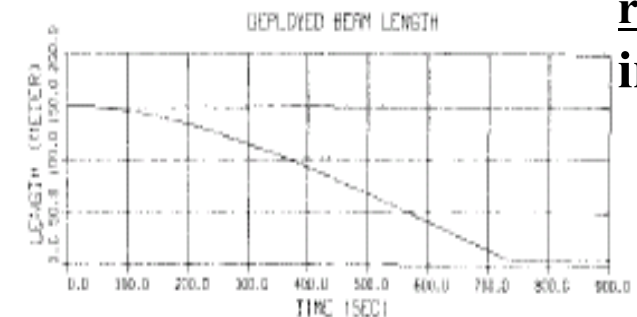
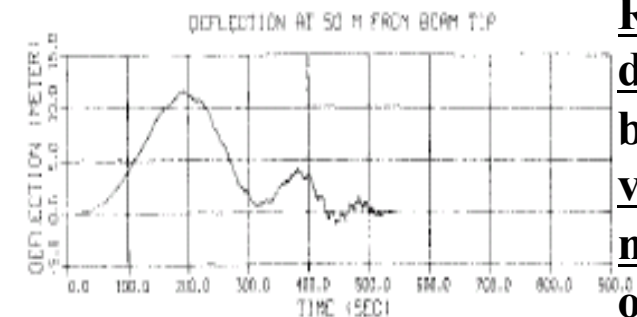
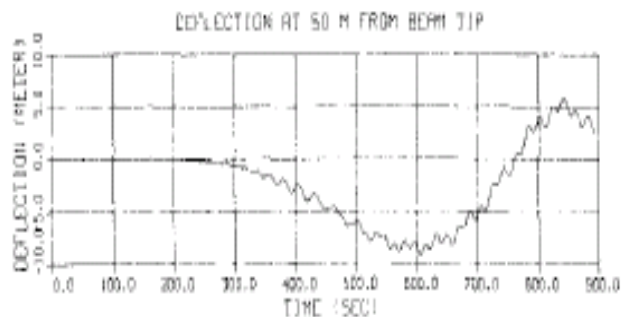
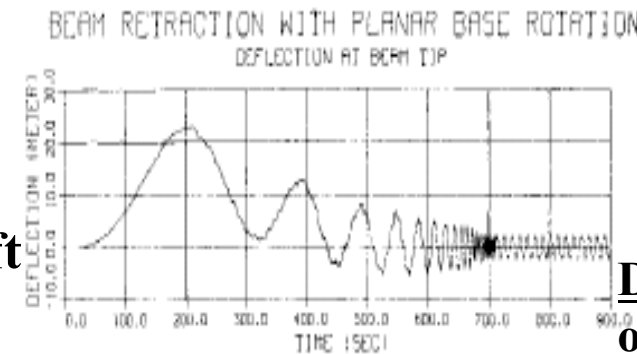
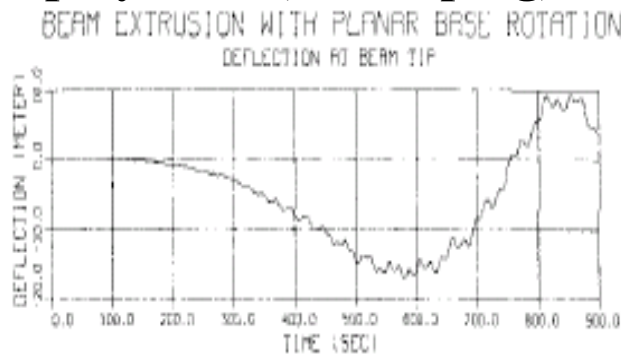
Tip
Deflec
max 23 ft

Deploying
or
Retrieval
described
by
varying
number
of
rigid rods
in play

Deflec
50 m
from
tip

12 min to
deploy/
retrieve
150 m
boom

Boom
Length



WISP Boom Bending due to Coriolis Force

Modeling Cable Deployment Dynamics in Towing of Underwater Powered Device Connected by Cable to Ship

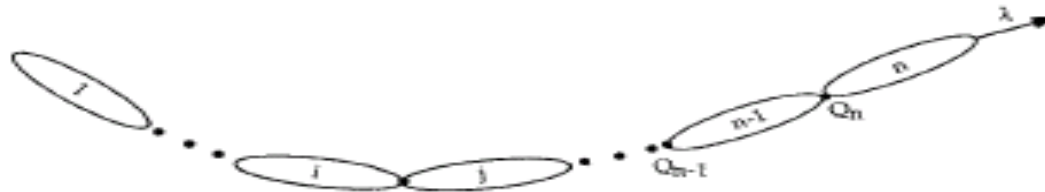
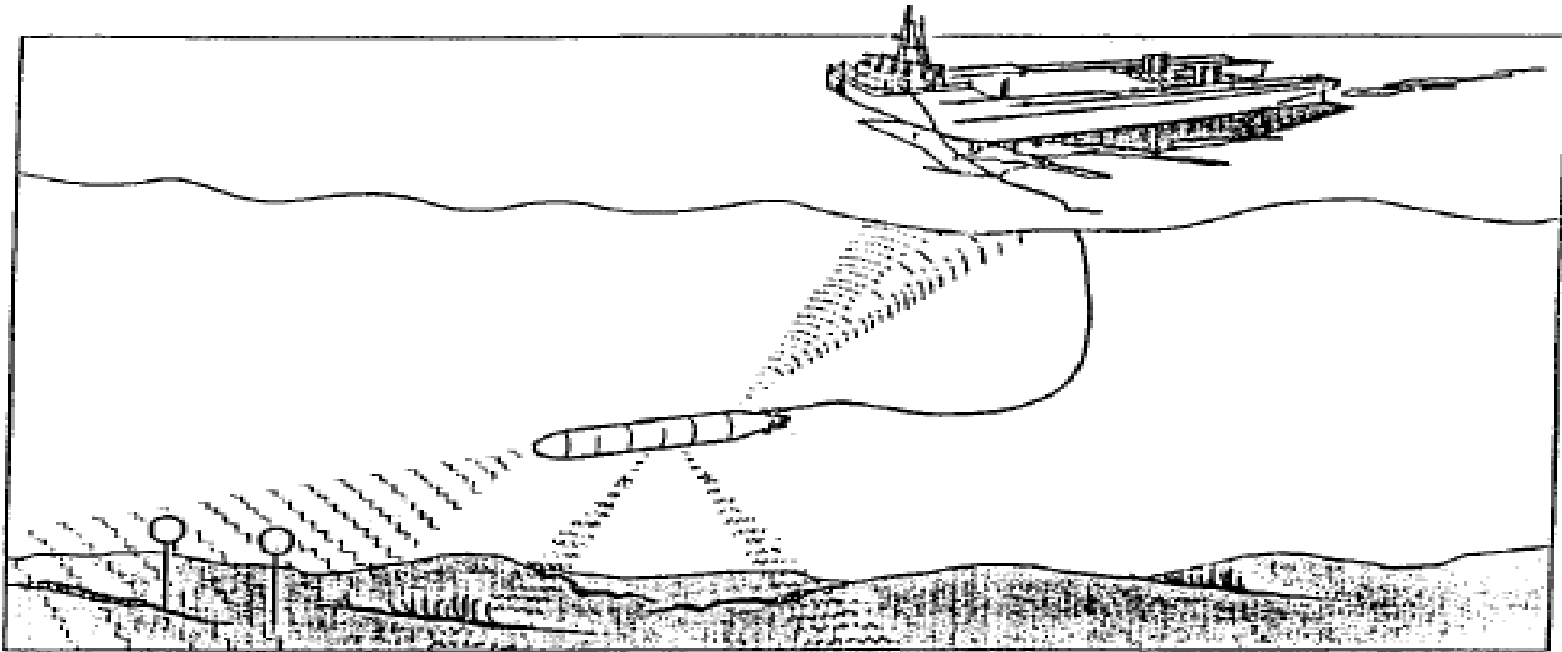


Fig. 2 Discretization of cable.

Cable modeled by
pinned links with
no joint stiffness:
Banerjee & Do,
JGCD, '94

Cable Length & Tension Change in Deployment / Retrieval vs. Time

deployment

600 m in 600 sec

retrieval

length

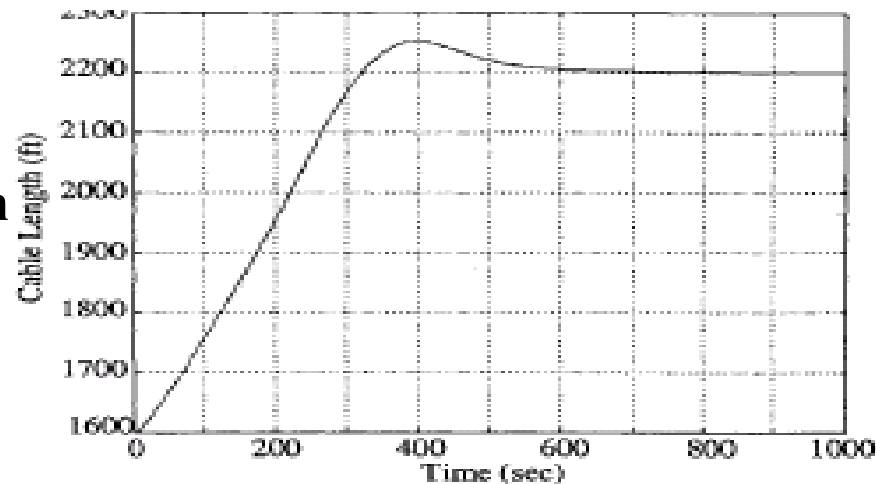


Fig. 7a Cable length vs time during deployment.

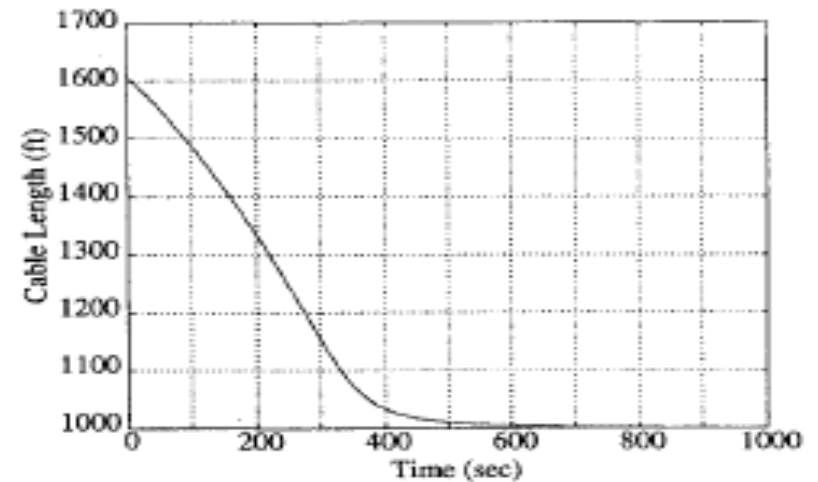


Fig. 9a Cable length vs time during retrieval.

tension

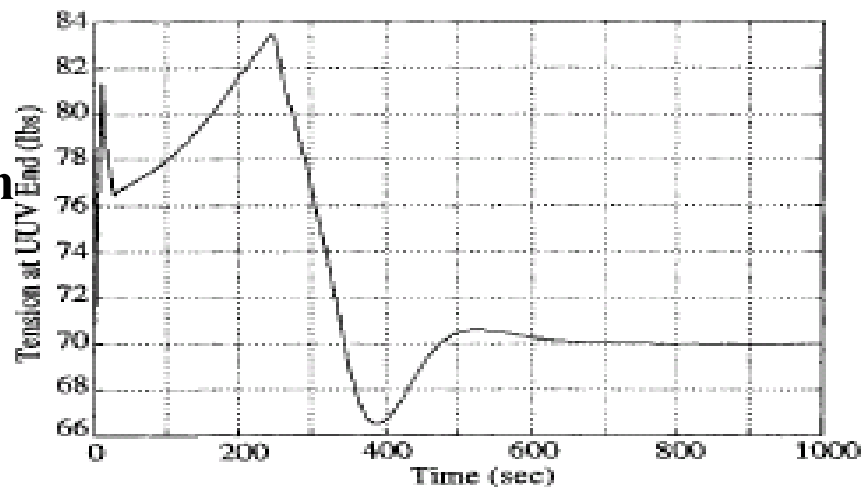


Fig. 7b Cable tension vs time during deployment.

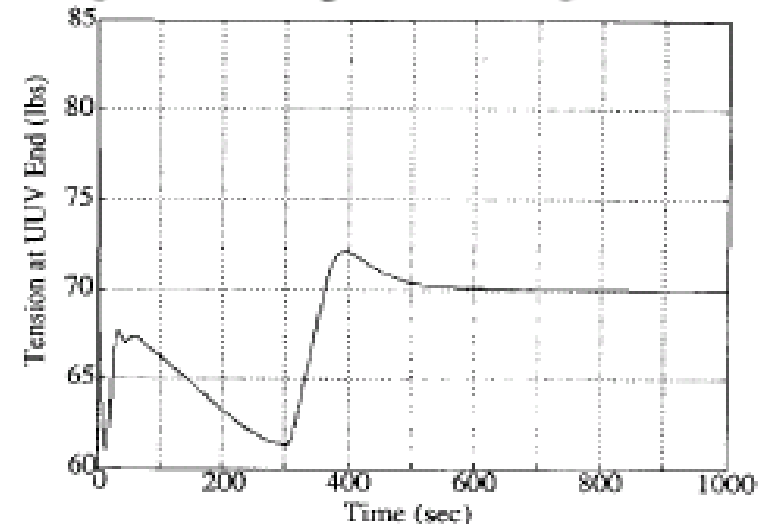
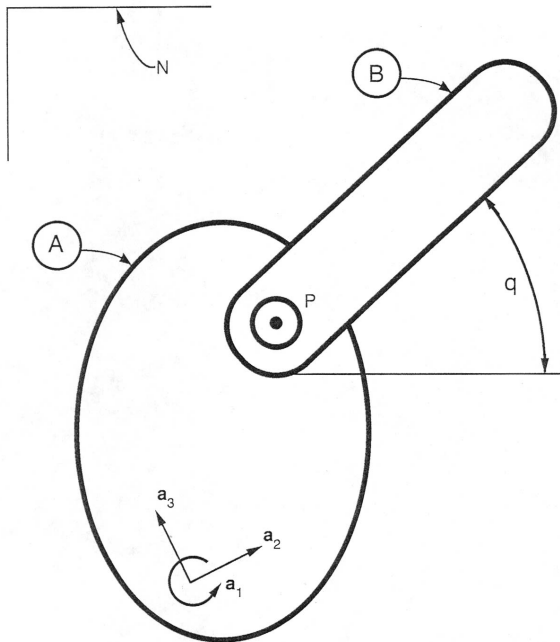


Fig. 9b Cable tension vs time during retrieval.

Monitoring internal force with $O(n)$ formulation

Simplifying Rotational Generalized Speeds (Mitiguy & Kane)

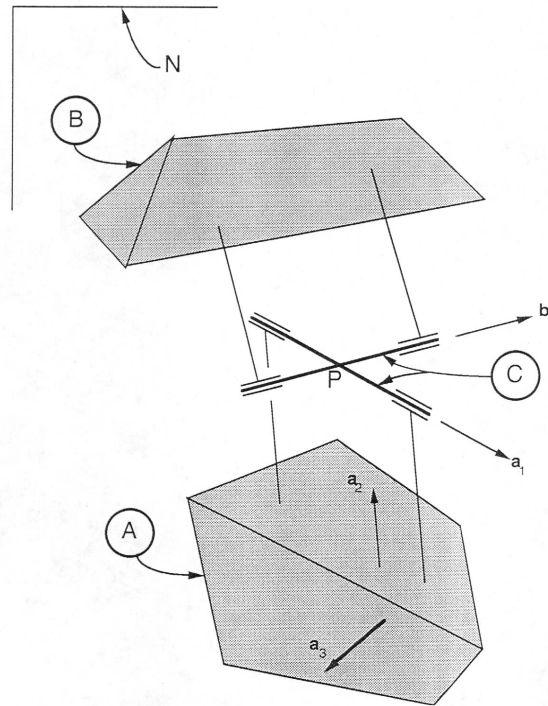
Revolute Joint



Generalized Speeds

$$u_1 = {}^N \boldsymbol{\omega}^B \cdot \mathbf{a}_1$$

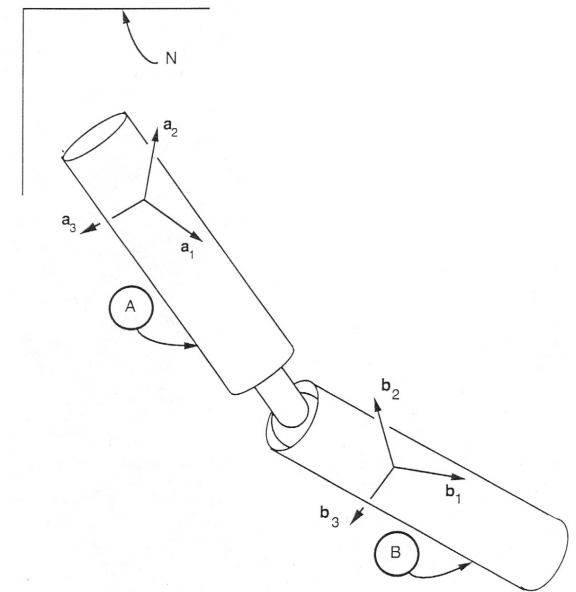
2 DOF Az-El Gimbal



$$u_1 = {}^N \boldsymbol{\omega}^C \cdot \mathbf{a}_1$$

$$u_2 = {}^N \boldsymbol{\omega}^B \cdot \mathbf{b}_2$$

3 DOF Spherical Joint

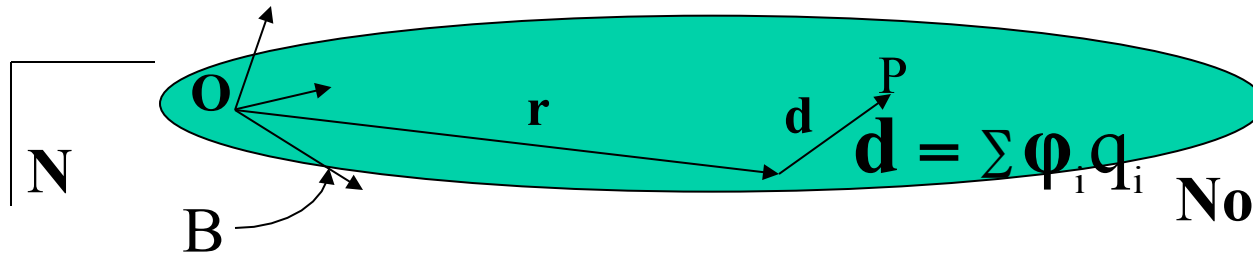


$$u_i = {}^N \boldsymbol{\omega}^B \cdot \mathbf{b}_i$$

$$(i = 1, 2, 3)$$

Hinge relative rotation angle rates are not the best choices

Efficient Generalized Speeds (D' Eleuterio & Hughes) for Vibration of Elastic Bodies in Large Rotation



Note: use of vibration modes, universally done, is an act of premature linearization

$${}^N \mathbf{V}^P = {}^N \mathbf{V}^O + {}^N \boldsymbol{\omega}^B \times (\mathbf{r} + \sum \phi_i q_i) + \sum \phi_i \dot{q}_i$$

Propose Gen. Speeds $\sigma_i \Rightarrow \sum_i \phi_i \sigma_i = {}^N \boldsymbol{\omega}^B \times \sum_i \phi_i q_i + \sum_i \phi_i \dot{q}_i$

$${}^N \mathbf{V}^P = {}^N \mathbf{V}^O + {}^N \boldsymbol{\omega}^B \times \mathbf{r} + \sum \phi_i \sigma_i$$

Velocity expression free of modal coordinates !

kinematics eqs: $\sum_i \int \phi_i \phi_j dm (\sigma_j - \dot{q}_j) = {}^N \boldsymbol{\omega}^B \times \sum_i \int \phi_j \phi_i dm q_j$

Consequences of q-independence of Velocity Expression on Mass Matrix in Kane's Equations for a Free-Flying Flexible Body

$$N_{\mathbf{v}}P = \sum_i^3 u_i \mathbf{b}_i + \sum_i^3 u_{3+i} \mathbf{b}_i \times \mathbf{r} + \sum_i^n \phi_i u_{6+i} \Rightarrow \frac{\partial N_{\mathbf{v}}P}{\partial u_i} \neq f(q) \quad , (i = 1, \dots, 6 + n)$$

Partial velocities are now free of generalized coordinates

Kane's Equations, obtained by integrating over body, are:

$$\int \sum_{j=1}^n \frac{\partial \mathbf{v}}{\partial u_i} \cdot \frac{\partial \mathbf{v}}{\partial u_j} dm \quad \dot{u}_j = - \int C \cdot \frac{\partial \mathbf{v}}{\partial u_i} dm - \sum \left[\frac{\partial P}{\partial q_j} + \frac{\partial D}{\partial \dot{q}_j} \right] \frac{\partial \dot{q}_j}{\partial u_i} + \sum_{k=1}^{NF} F_k^{ext} \cdot \frac{\partial \mathbf{v}^k}{\partial u_i} \quad (i = 1, \dots, 6 + n)$$

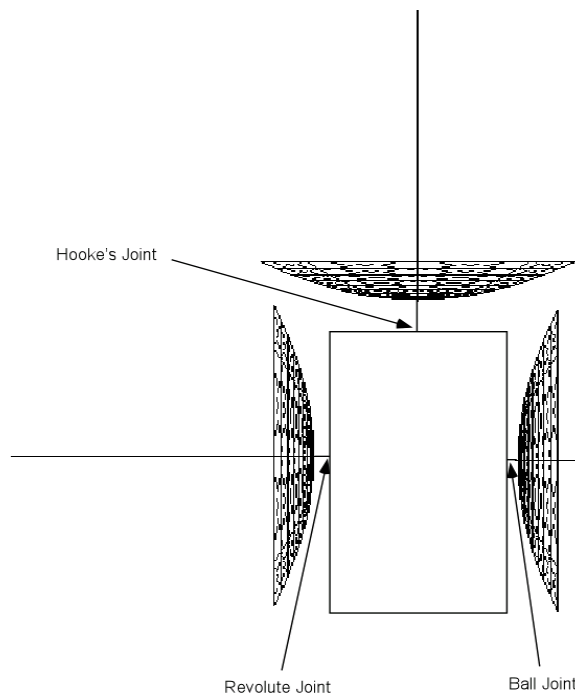
$$M \dot{U} = R$$

Mass matrix in LHS is now constant

Facilitates fast computation for single or terminal flexible body.

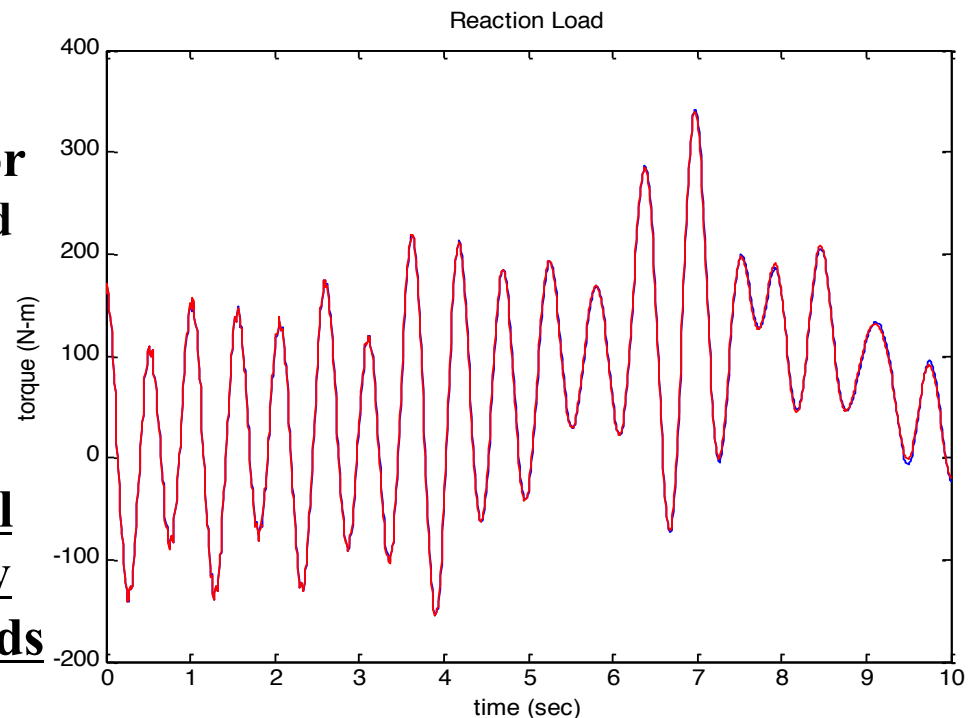
Application: System of 4 Hinge-Connected Flexible Bodies, Kane's vs. Recursive Method with Efficient Gen. Speeds--- Loads Analysis

Constraint torque at a joint in a 4-flex-body system with 1-, 2-, 3-rotation joints: [Int. Cong. Theo. & App. Mech, Warsaw, 04]



Internal
torque for
prescribed
motion of
rev. joint

Identical
result by
2 methods



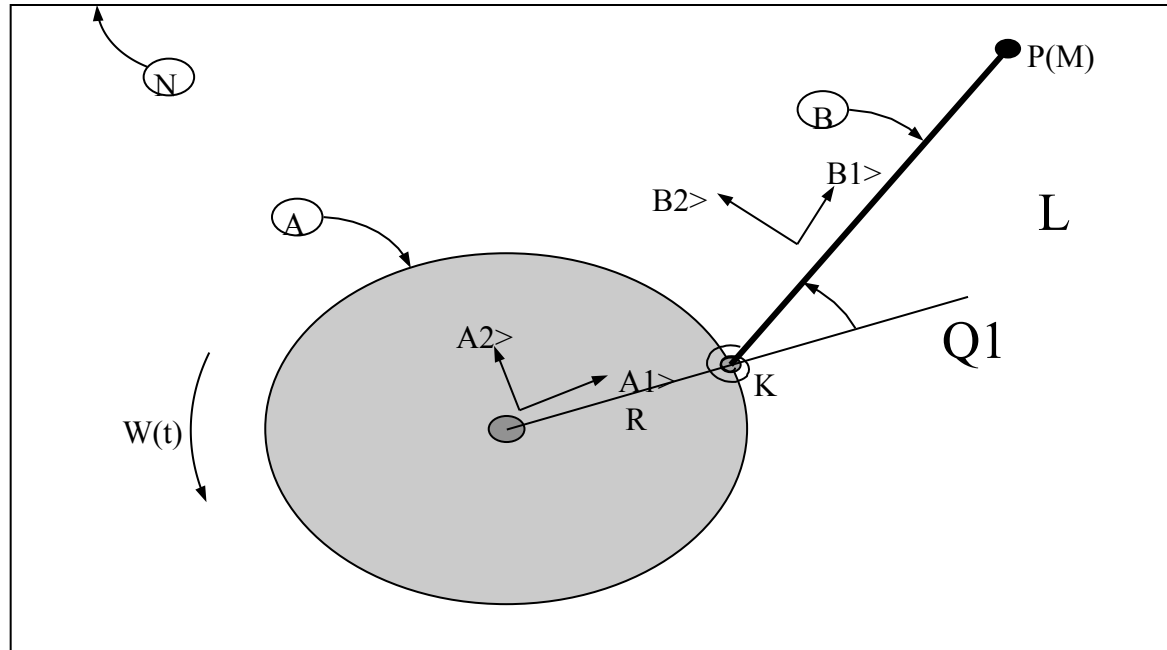
Kane's Eqns with customary generalized speeds

44.4 sec

Recursive Eqns with efficient generalized speeds

21.0 sec

Perils of Premature Linearization for Small Motion : Use of Vibration Modes, Can Lead to Loss of Stiffness



Premature linearization occurs if partial velocity in Kane's eqn is derived from linear velocity. Recall Kane's Eqns:

$$0 = \sum_{k=1}^{NP} [F^k + (-m^k \mathbf{a}^k)] \cdot \frac{\partial \mathbf{v}^k}{\partial \mathbf{u}_i}, i = 1, \dots, n$$

Linearized velocity of P in N for small angle Q1

$$LVPN> = -\Omega * L * Q1 * A1> + ((L+R) * \Omega + U1 * L) * A2>: \quad \mathbf{PV}> =: L * A2>$$

$$LACC> = (...) * A1> + ((L+R) * \Omega' + U1' * L - \Omega^2 * L * Q1) * A2>$$

$$M * LACC> . \mathbf{PV}> = -K * Q1 \quad (\text{Kane's Eqn})$$

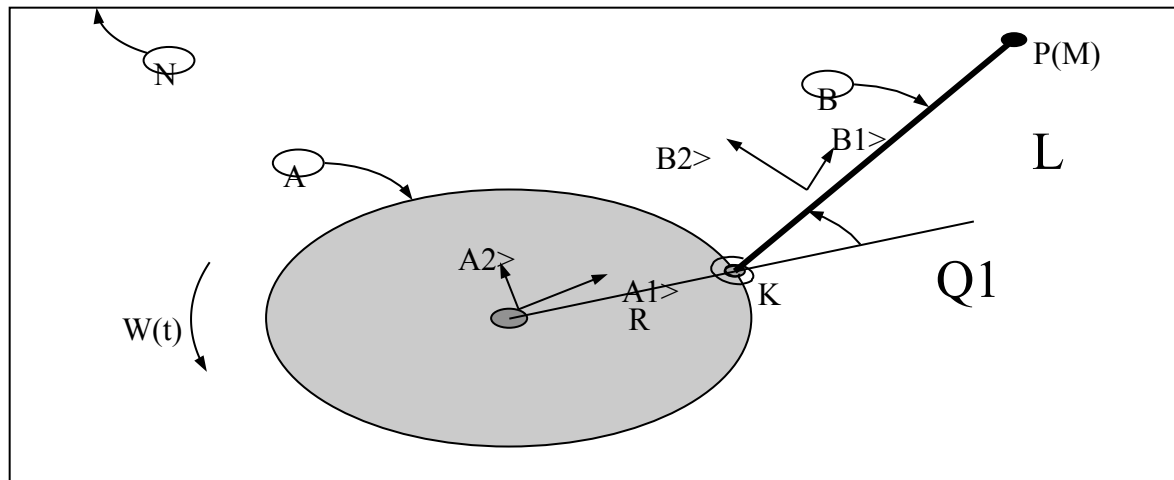
$$U1' = -[K / (M * L^2) - \Omega^2] * Q1 - (1 + R/L) * \Omega'$$

wrong eqn !

Stiffness decreasing with speed, possibly going negative !

Correct Linearization Without Deriving Full Nonlinear Equations

Small vibration of pendulum with large base rotation



***Linearize partial velocity from nonlinear velocity expression.**

(Beam paper: Kane, Ryan & Banerjee, JGCD, '87; Plate Paper: Banerjee & Kane, JAM, '89)

Nonlinear expression of velocity of P in N

$$NLVPN> = \Omega * R * A2> + (\Omega + U1) * L * (-\sin(Q1) * A1> + \cos(Q1) * A2>)$$

$$PVN> = L * (-\sin(Q1) * A1> + \cos(Q1) * A2>);$$

Now linearize: $LPV> = L * (A2> - Q1 * A1>)$ **Premature. linear par. vel $PV> =: L * A2>$**

$$LVPN> = -\Omega * L * Q1 * A1> + ((L+R) * \Omega + U1 * L) * A2>$$

$$ACC> = -A1> * (.. + (L+R) * \Omega^2) + ((L+R) * \Omega' + L * (U1' - \Omega^2 * Q1)) * A2>$$

$$U1' = -[K / (M * L^2) + (R/L) * \Omega^2] * Q1 - (1 + R/L) * \Omega'$$

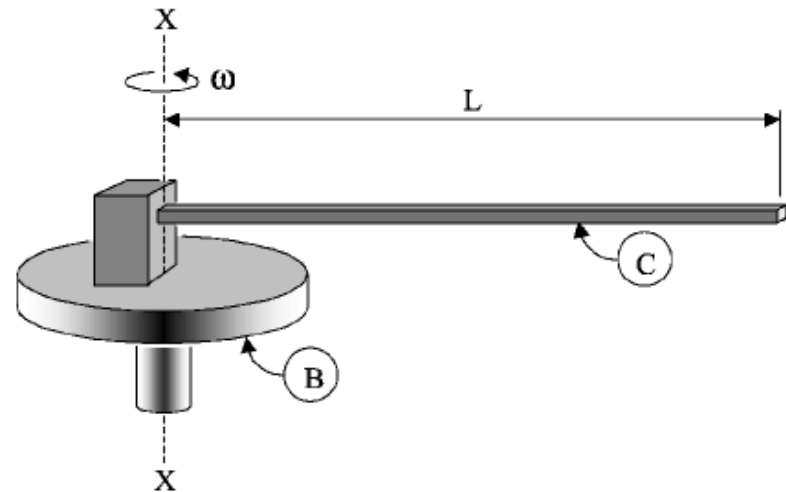
correct eqn

***This approach is not feasible for general elastic continua.**

Spin-up Maneuver of Attached Base

Good Test Case for Centrifugal Stiffening of Beams, Plates, and Arbitrary Flexible Structures: Spin-up Maneuver of the Attached Base

$$\omega = \frac{\Omega}{T} \left[t - \frac{T}{2\pi} \sin \frac{2\pi t}{T} \right], \quad t < T$$
$$= \Omega, \quad t > T$$



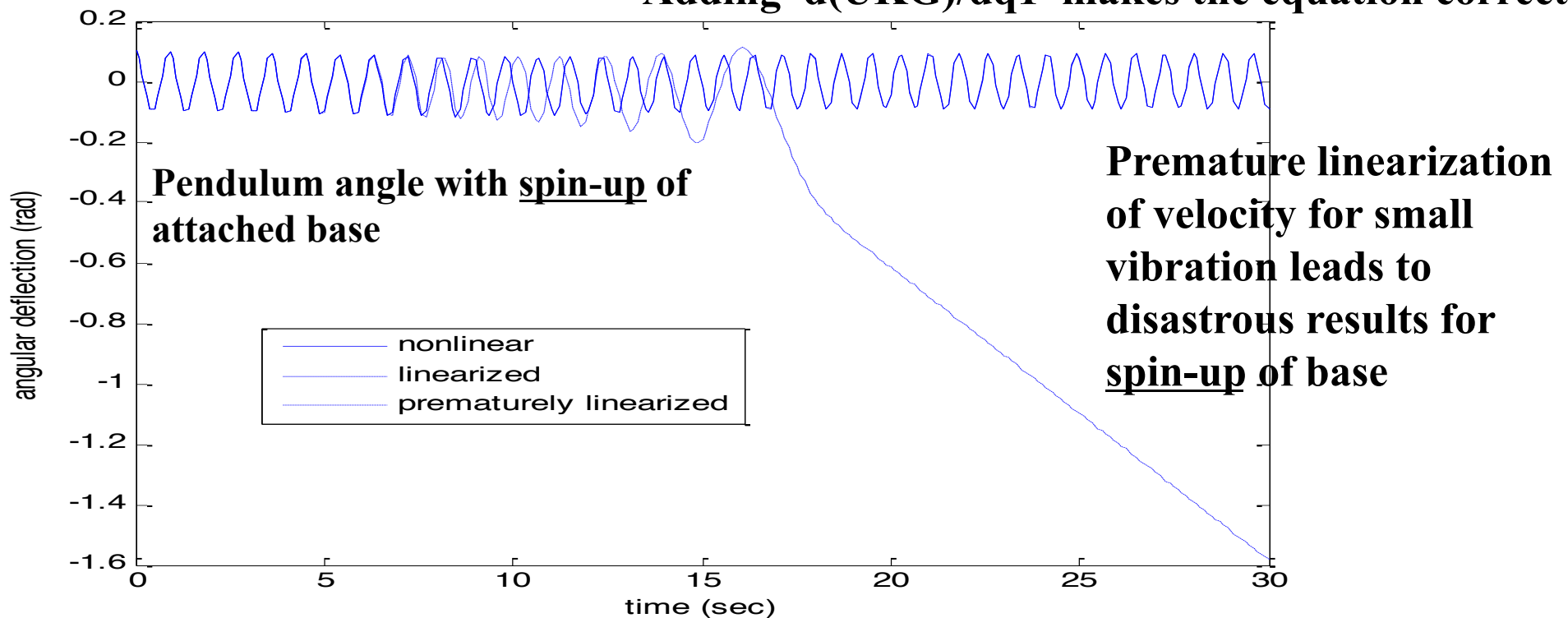
Relevant for Helicopter Rotor Spin-up & Steady Spin

Redeeming Prematurely Linearized Eqns by Adding Geometric Stiffness due to Inertia Loads: Makes Up for Loss of Stiffness

$$UKG = 0.5 * M * \Omega^2 * (R+L) / L * [0, q_1] * [1; -1; -1, 1] * [0; q_1] \quad \text{Potential for KG of bar* due to inertia load}$$

$$U1' = [-K / (M * L^2) + \Omega^2 - \frac{(1+R/L) * \Omega^2}{L}] * q_1 - (1+R/L) * \Omega^2$$

Adding $d(UKG)/dq_1$ makes the equation correct



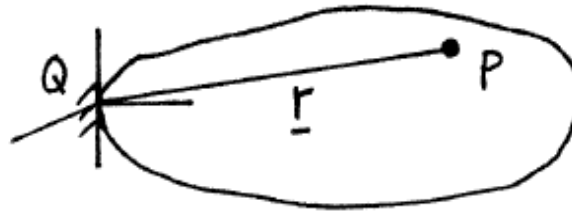
$$UKG = \frac{AE}{2} \int_0^L \left[\frac{\partial u_x}{\partial x} \right]_0 \left(\frac{\partial u_y}{\partial x} \right)^2 dx = [q_1 \quad q_2] \left(\frac{F}{L} \right) \begin{bmatrix} 1 & -1 \\ -1 & 1 \end{bmatrix} \begin{Bmatrix} q_1 \\ q_2 \end{Bmatrix}$$

[Przemieniecki]*

USING VIBRATION MODES IN LARGE OVERALL MOTION IS AN ACT OF PREMATURE LINEARIZATION: A GENERAL THEORY OF MOTION-INDUCED STIFFNESS CORRECTS UNAVOIDABLE ERROR IN EQUATIONS

BANERJEE & DICKENS USES PRECOMPUTED GEOMETRIC STIFFNESS DUE TO BASE ACCELERATION FOR GENERAL CONTINUA

$$a^P = a^Q + \tilde{\alpha} r + \tilde{\omega} \tilde{\omega} r$$



$$\begin{Bmatrix} f_1 \\ f_2 \\ f_3 \end{Bmatrix} = -dm \begin{bmatrix} 1 & 0 & 0 & x & 0 & 0 & y & 0 & 0 & z & 0 & 0 \\ 0 & 1 & 0 & 0 & x & 0 & 0 & y & 0 & 0 & z & 0 \\ 0 & 0 & 1 & 0 & 0 & x & 0 & 0 & y & 0 & 0 & z \end{bmatrix} \begin{Bmatrix} a_1 \\ a_{12} \end{Bmatrix}$$

Compute KG from FEM for inertia load on a point mass at (x,y,z)

$$F = - \sum_{i=1}^{12} a_i \Phi^T K_i^g \Phi \eta$$

Gen. force for motion-induced stiffness

Add geometric stiffness for 12 sets of motion-induced loads, for general motion of frame, to overcome loss of stiffness inevitably occurring with use of vibration modes

“Dynamics of an Arbitrary Flexible Body in Large Rotation and Translation” by Banerjee & Dickens, JGCD, '90, where acceleration terms, a_1, \dots, a_{12} are identified. See results on next slide:

BEAM & PLATE SPECIAL THEORIES COMPARED AGAINST GENERAL THEORY WITH MOTION-INDUCED STIFFNESS : case of BASE SPIN-UP

Cantilever beam, Freq 1 = 0.546R/s, Omega = 0.76R/s, T = 1200 s

Cantilever plate, Freq 1 = 0.75R/s, Omega 1 = 1.25R/s T = 30 s

Beam
tip defln
by two
theories

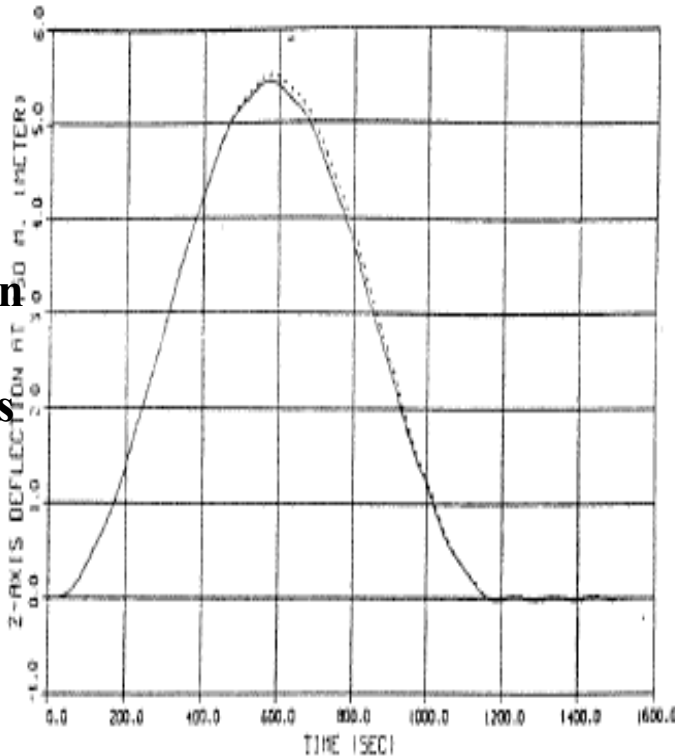
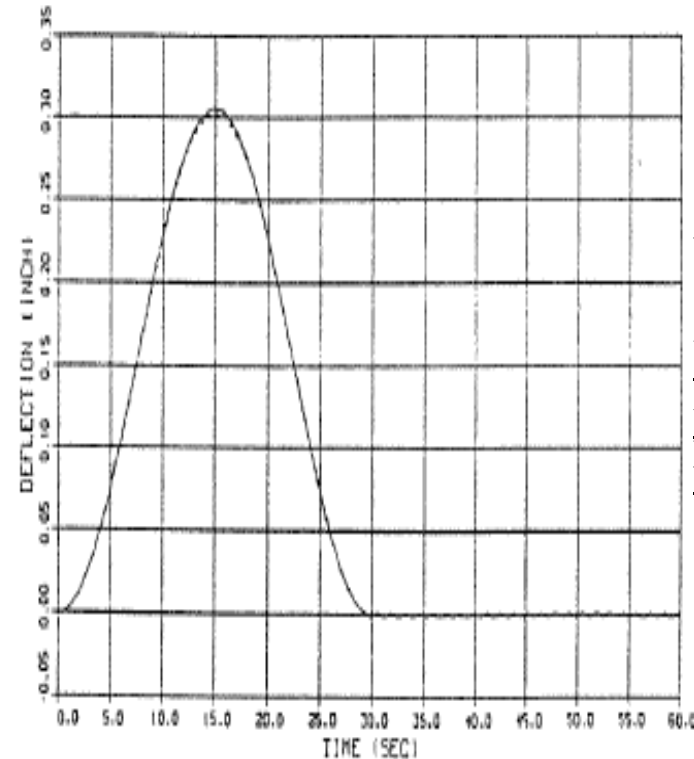


Plate
corner
defln
by two
theories



Geo. stiff.
theory
& special*
beam and
plate
theories
agree

Fig. 6 Cantilever beam tip deflection during spin-up given by the present theory (solid line) and the theory of Ref. 1 for steady-state spin frequency greater than the first vibration mode frequency.

Fig. 7 Cantilever plate corner deflection during spin-up given by the present theory (solid line) and the theory of Ref. 3 for steady-state spin frequency greater than the first vibration mode frequency.

*Beam neutral axis stretches [JGCD,' 87]

*Plate midsurface does not stretch[JAM,' 89]

Flexible Spinning Paraboloidal Antenna of Dual-Spin Spacecraft

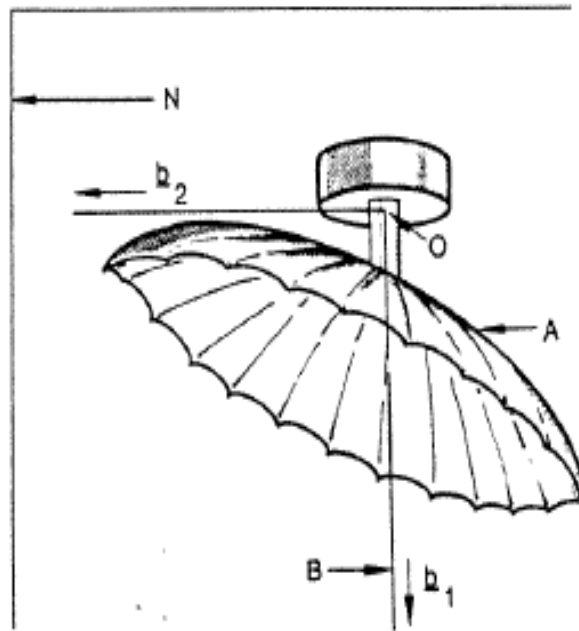


Fig. 1 Dual-spin spacecraft with flexible, spinning offset paraboloidal antenna.

Shell
node
defln in
spin-up
by two
theories

Paraboloidal antenna, Freq 1 = 0.433 Hz, Omega = 0.5 Hz, T = 30 s

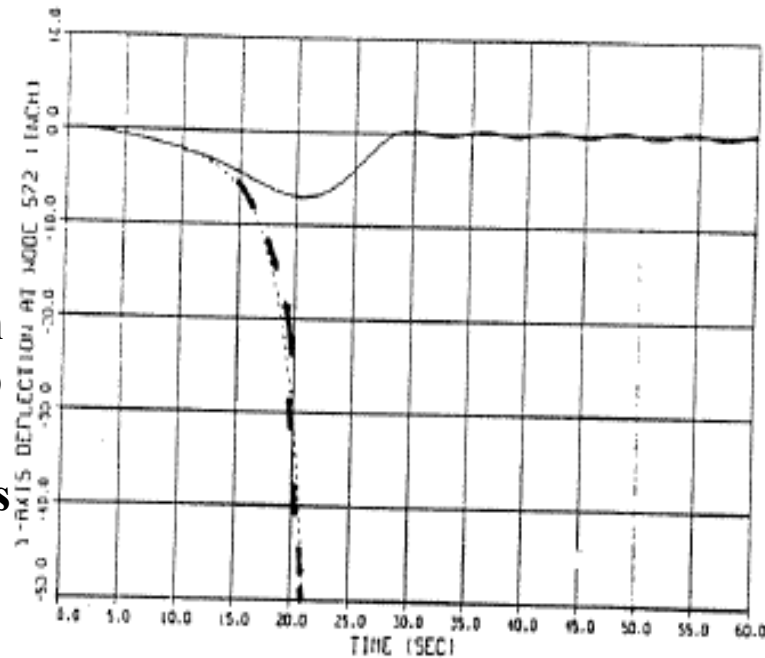
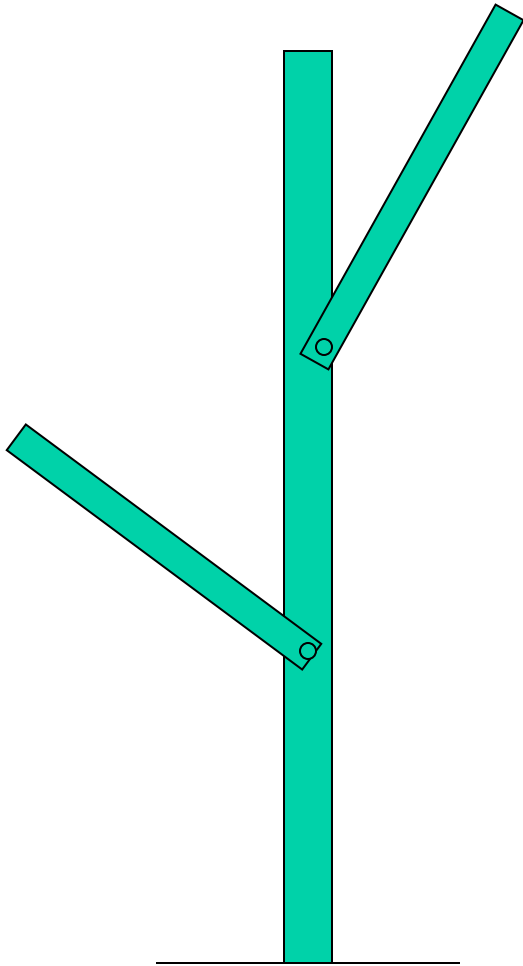


Fig. 2 Elastic displacement along y axis at a finite-element node of paraboloidal antenna for spin-up given by present theory (solid line) and a conventional theory (dashed line); steady-state spin frequency is greater than the first mode vibration frequency.

Spin-up of paraboloid shell model: KG-theory works, modal theory fails [Banerjee & Dickens, JGCD, '90, pp. 221-227]

Model Reduction for Articulated Flexible Bodies : 3 Beam Example



- Three hinge-connected elastic beams with actuator and sensor at joints

$$\mathbf{M} \begin{Bmatrix} \ddot{q}_1 \\ \ddot{\theta}_1 \\ \ddot{q}_2 \\ \ddot{\theta}_2 \\ \ddot{q}_3 \end{Bmatrix} + \mathbf{K} \begin{Bmatrix} q_1 \\ \theta_1 \\ q_2 \\ \theta_2 \\ q_3 \end{Bmatrix} = \begin{Bmatrix} \\ \\ \\ \\ \end{Bmatrix} \{u\}$$

We want to select a set of component modes that participate significantly in the system modes

Flexible Body Model Reduction by Singular Value Decomposition of Projected SYSTEM Modes: Three Beam Example

Elastic deformation given by component modes times modal coord

$$\delta_1 = \phi_1 q_1, \delta_2 = \phi_2 q_2, \delta_3 = \phi_3 q_3$$

Component modal coordinates related to system modal coordinates

$$\begin{Bmatrix} q_1 \\ \theta_1 \\ q_2 \\ \theta_2 \\ q_3 \end{Bmatrix} = \begin{bmatrix} A \\ B \\ C \end{bmatrix} \{\eta\};$$

A, B, and C are projections of system eigenvectors on component modal coordinate subspace

$$[U_1, \Sigma_1, V_1] = \text{svd}(A); \quad [U_2, \Sigma_2, V_2] = \text{svd}(B); \text{ etc.}$$

$$\delta_1 = \phi_1 \hat{U}_1 \eta_1 = \hat{\phi}_1 \eta_1; \quad \delta_2 = \phi_2 \hat{U}_2 \eta_2 = \hat{\phi}_2 \eta_2; \quad \text{etc.}$$

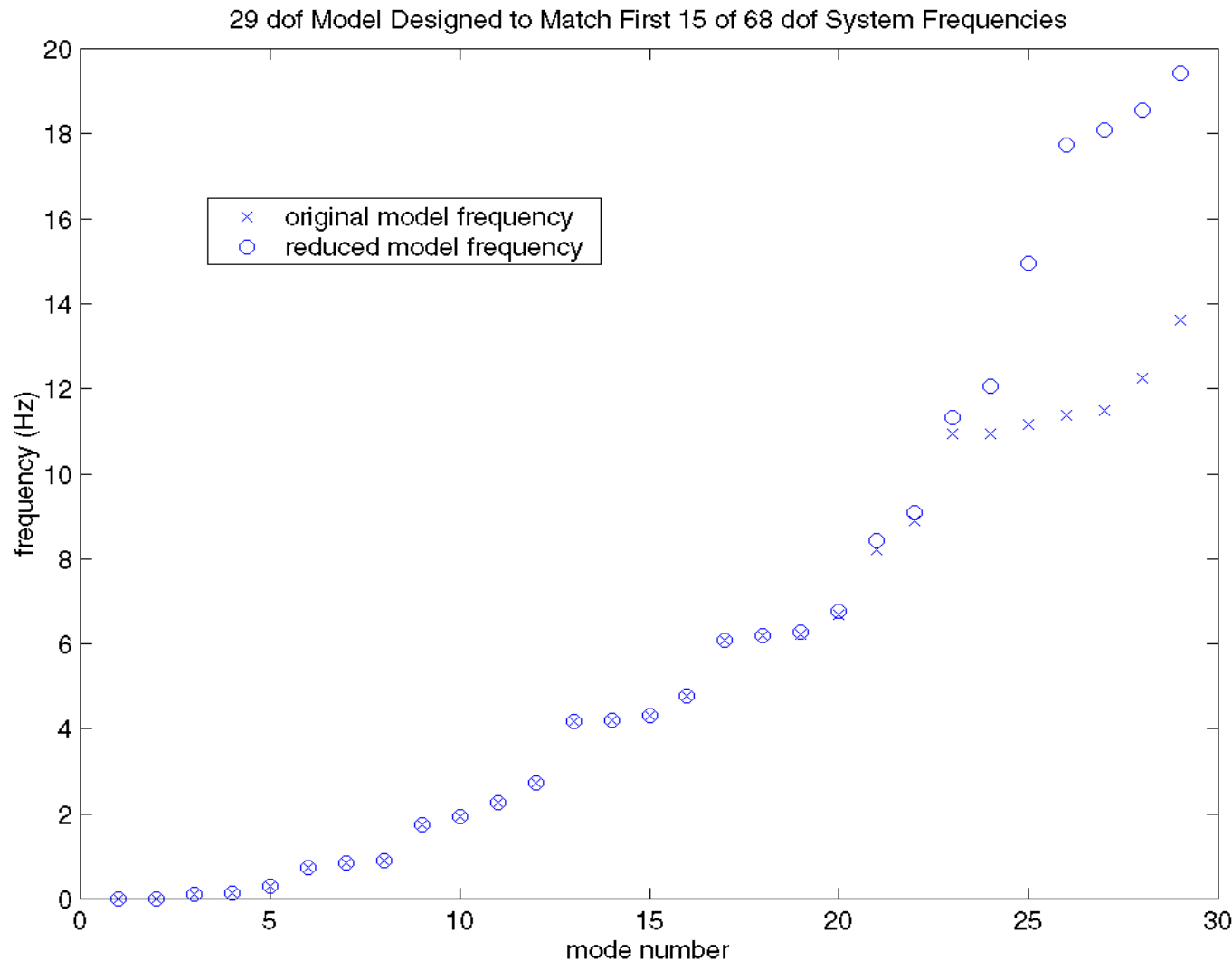
$$q_1 = A \eta$$

$$q_2 = B \eta$$

$$q_3 = C \eta$$

Do SVD of A,B,C and keep as many columns of U as the ranks (SV) of A,B,C to modify comp modes

Results of 29 dof model designed to match first 15 freqs of 68 dof articulated flexible body system for 3 beam model [Lemak]



$$\delta_1 = \phi_1 \hat{U}_1 \eta_1$$

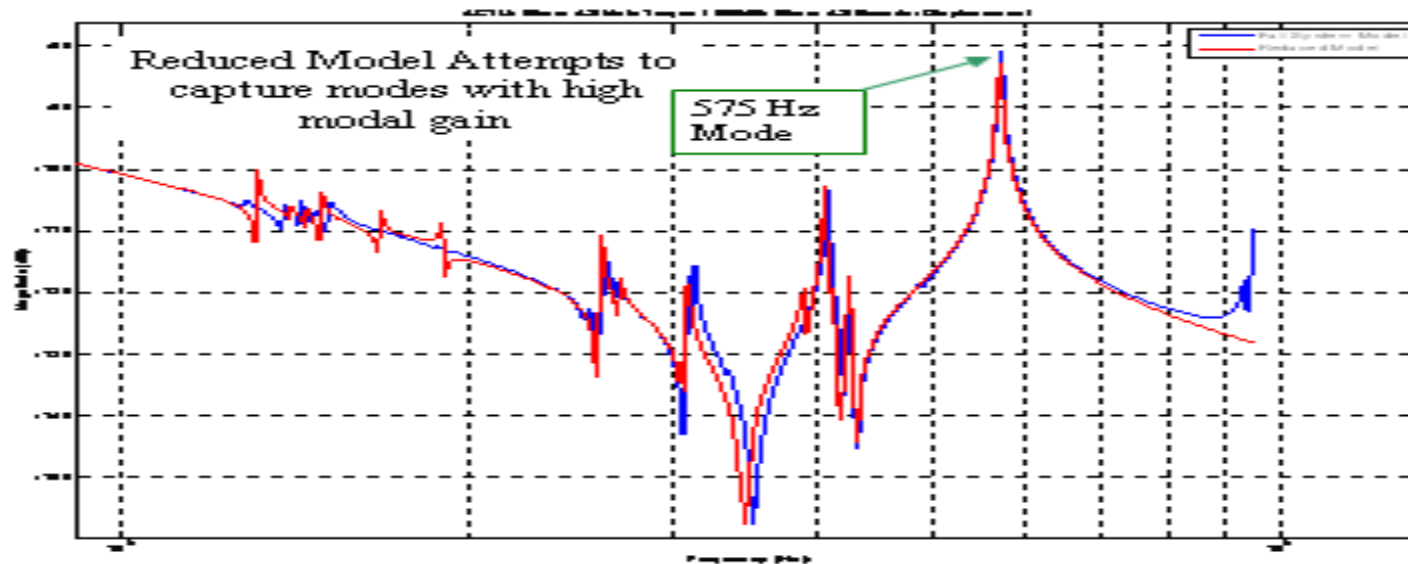
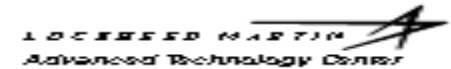
$$\delta_2 = \phi_2 \hat{U}_2 \eta_2$$

$$\delta_3 = \phi_3 \hat{U}_3 \eta_3$$

Out of 15 system modes, SVD kept 15 modes in matrix A of body 1, 5 modes in B of body 2, and 9 modes in C of body 3, to get a (15+5+9)dof model

Bode Plot for Reduced & Full Order Model in An Actual Application [Lemak]

High Frequency Torque to Angle Displacement Bode Response



Precision Pointing & Controls

Lockheed Martin Proprietary Information

03/22/05 Chart 21

Body	SC Bus	Scan. Pivot Tube	Scan. Mirror	Scan. Az Wheel	Scan. El Wheel	Starer Pivot Tube	Starer Mirror	Starer Az Wheel	Starer El Wheel
Full System Modes	*894	30	9	3	3	30	9	3	3
<u>Reduced Model Modes</u>	*31	4	2	3	3	4	2	3	3

03/22/05 Chart 27

Deriving Damping of Components from System Level Damping

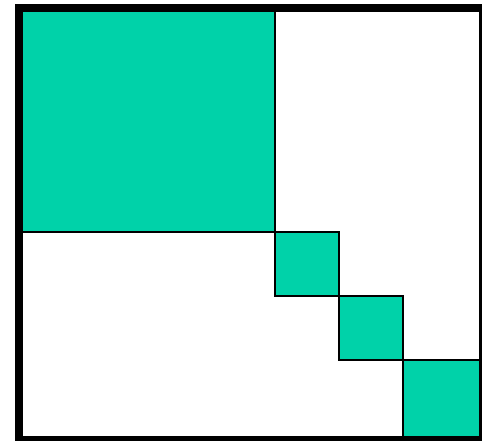
Assume System Damping Factor ζ

$$C = \Phi^{-t} [2 \zeta \omega] \Phi^{-1}$$

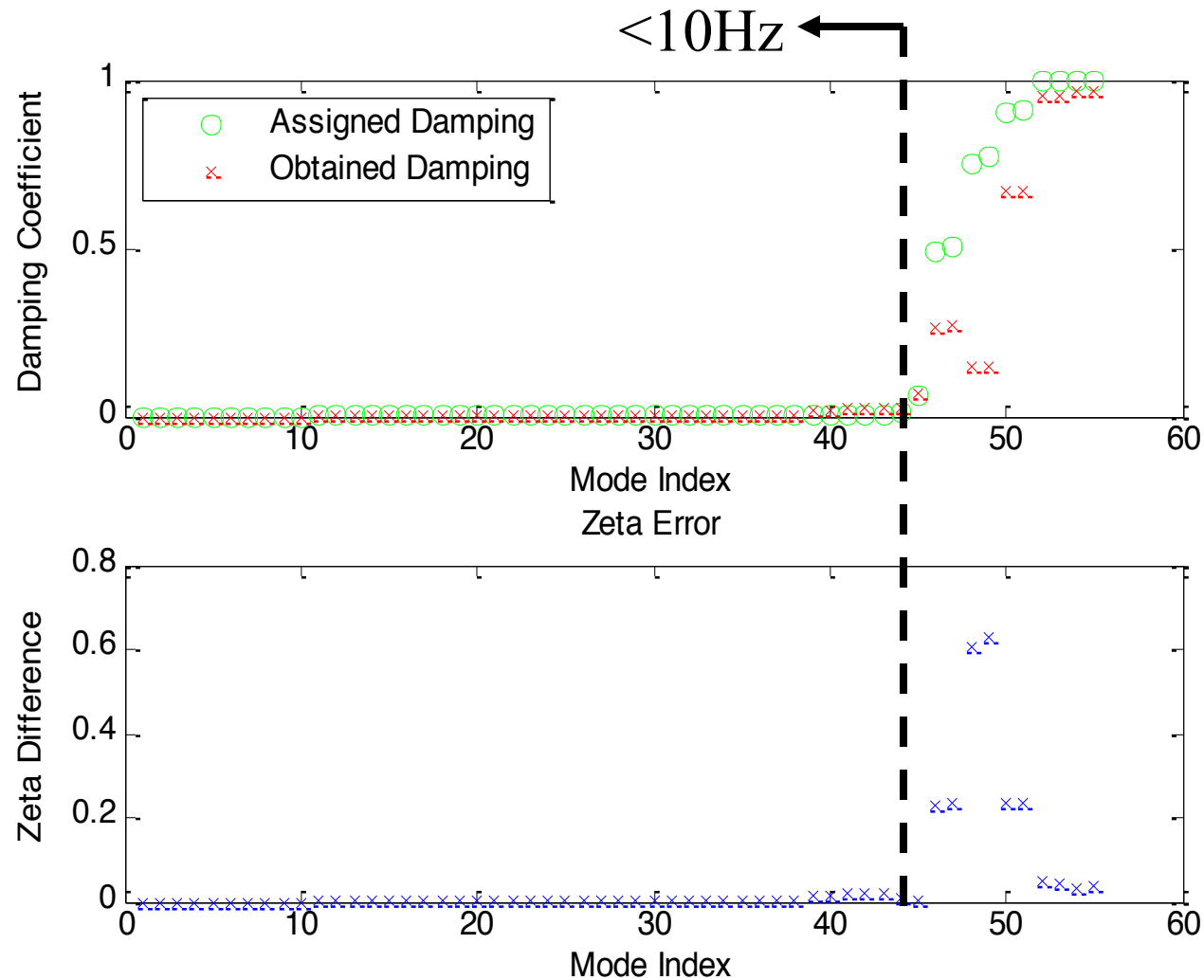
$$\Phi^{-1} = (\Phi^t \Phi)^{-1} \Phi^t \quad \text{pseudo-inverse} \\ \text{least square err}$$

Derive component damping matrix,
with S_j matrix selecting component j

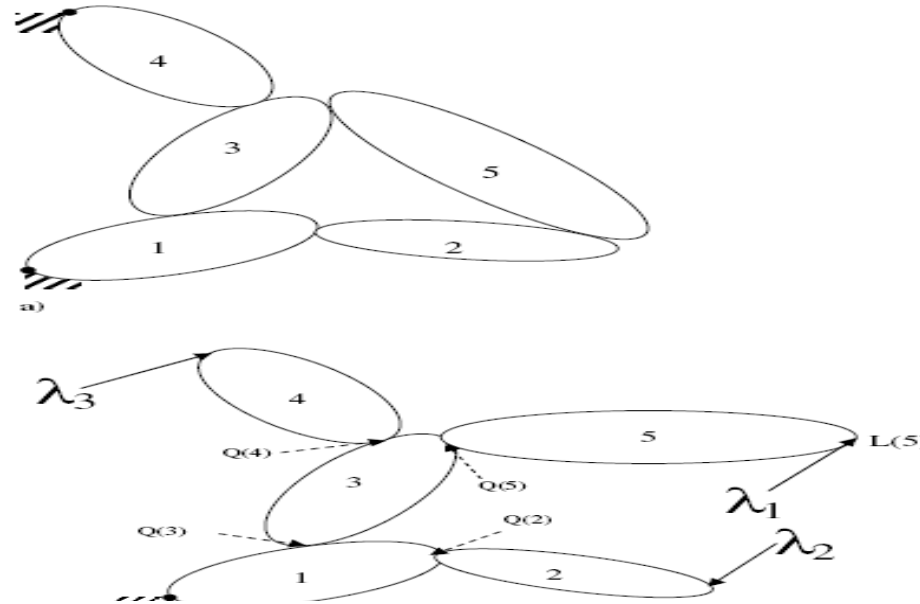
$$c_j = S_j C S_j^t$$



Result of System Damping Re-synthesis with Derived Component Damping in an Application [Lemak]



Recursive Formulation for Constrained Mechanical Systems

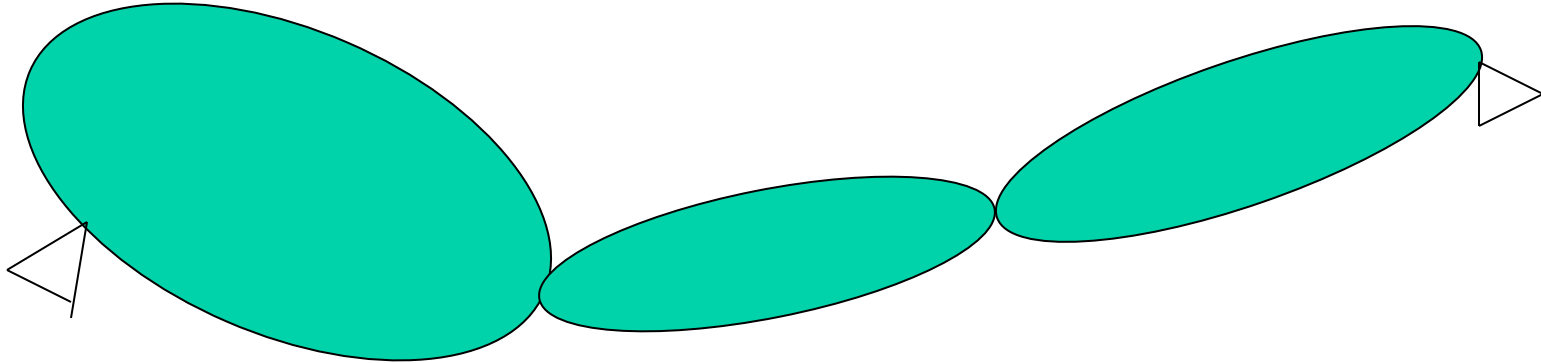


Closed loop system is cut to form open loop tree system: then add constraints.

1. Cut Loops and Make Forward Pass for Kinematics of Tree System so Formed
2. Do Backward Pass Tracking Part of Contributions from Constraint Forces
3. Complete Second Forward Pass with Constraint Forces in Dynamical Eqns
4. Add Constraint Conditions & Solve Dynamical & Constraint Eqns

Efficient Generalized Speeds, Recursive Formulation, and Multi-Point Constraints in Flexible Multibody Dynamics-Banerjee & Lemak, JGCD, '07

Constrained Dynamical Equations: Adding Extra DOFs and Constraint Eqns --- Two Formulations



Order- n^3 Extended Kane Eqns

New Order-n Eqns:

Both methods expose constraint force by cut & use constraint eqns

$$\begin{bmatrix} m_1 & m_2 & m_3 & a^t \\ m_2^t & m_4 & m_5 & b^t \\ m_3^t & m_5^t & m_6 & c^t \\ a & b & c & 0 \end{bmatrix} \begin{bmatrix} \dot{u}_1 \\ \dot{u}_2 \\ \dot{u}_3 \\ \lambda \end{bmatrix} = \begin{bmatrix} f_1 \\ f_2 \\ f_3 \\ d \end{bmatrix}$$

$$\begin{bmatrix} \dot{u}_1 \\ \dot{u}_2 \\ \dot{u}_3 \end{bmatrix} = \begin{bmatrix} g_1 \\ g_2 \\ g_3 \end{bmatrix} + \begin{bmatrix} h_1 \\ h_2 \\ h_3 \end{bmatrix} \{\lambda\}$$

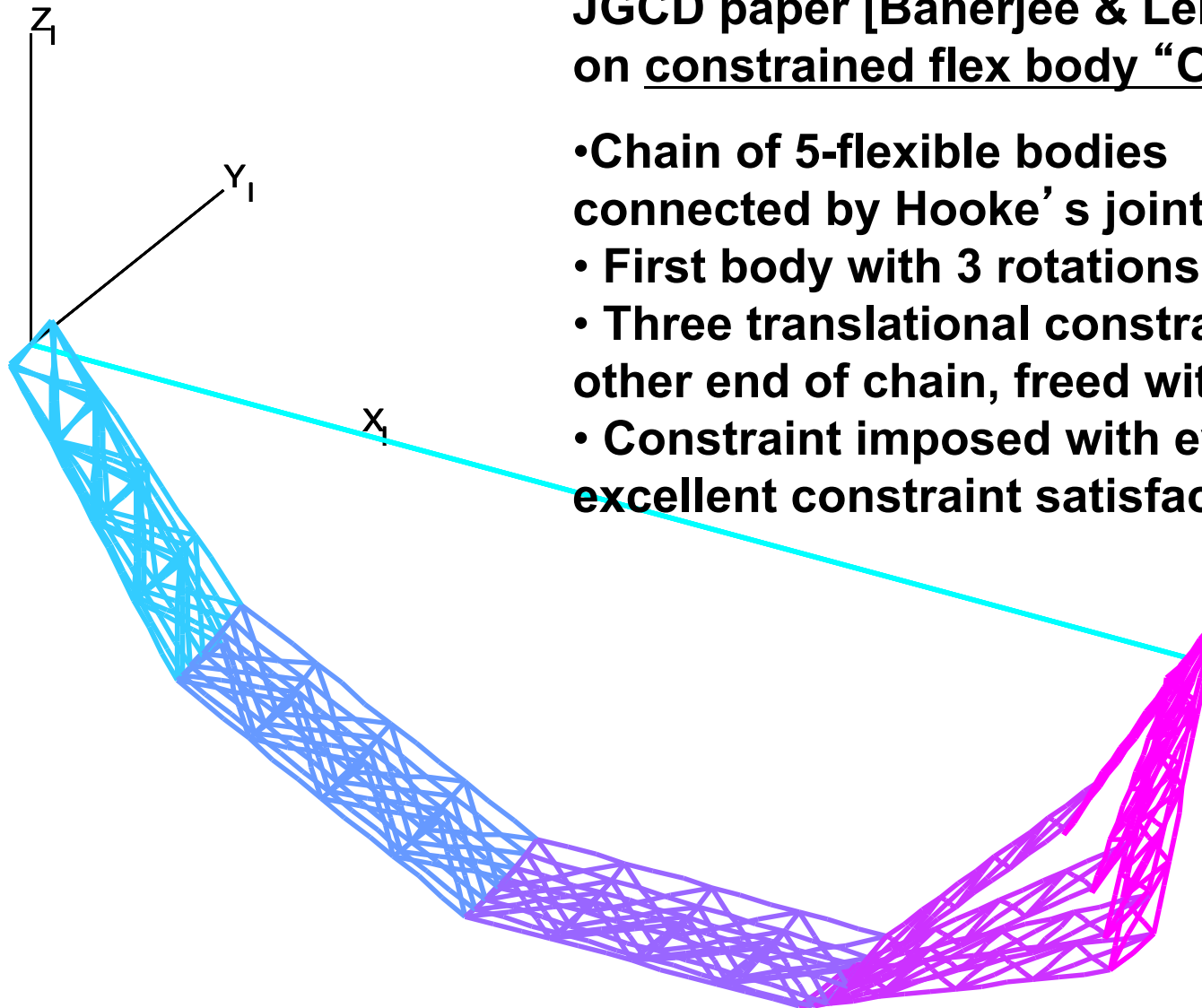
$$a\dot{u}_1 + b\dot{u}_2 + c\dot{u}_3 = d$$

CPU Results for 8 Bodies, 3 LOOPS, Varying # Modes [Lemak]

***Note: Absolute CPU time will go down with use of faster computers**

Number of Modes per Body	Number of Generalized Speeds	CPU sec for 10 sec Extended Kane Formulation*	<u>Ratio of Ext. Kane over Efficient Order-n Formulation</u>
0	24	6.28	0.969
4	56	57.57	1.516
8	88	909.29	3.053
12	120	2484.3	4.455

Stroboscopic Plot of a Whirling Chain of Five Articulated Elastic Trusses, 75 dof with 3 constraints [Lemak]



JGCD paper [Banerjee & Lemak, '07]
on constrained flex body “ $O(n)$ ” eqns

- Chain of 5-flexible bodies connected by Hooke's joint
- First body with 3 rotations
- Three translational constraints at other end of chain, freed with force
- Constraint imposed with eventual excellent constraint satisfaction

Kane's Equations for Variable Mass Flexible Body Dynamics

[Banerjee, Int. Cong. Th. & App. Mech, '08, Adelaide]

$$\int_0^{m(t)} {}^N \mathbf{v}_i^P \cdot {}^N \mathbf{a}^P dm =$$

$$\sum_{k \in L} {}^N \mathbf{v}_i^k \cdot (- \dot{m}_k \mathbf{v}_e) + \int_S {}^N \mathbf{v}_i^P \cdot d\mathbf{f}_{ext}$$

Thrust term

$$- \frac{\partial \pi}{\partial q_i} - \frac{\partial D}{\partial \dot{q}_i} ; i = 1, \dots, 6 + n$$

RHS has Thrust, External Forces, & Forces from Potential π due to Structural Stiffness & Geometric Stiffness due to Thrust, & Dissipation Functions D .

Form of (6+n) DOF Flexible Rocket Dynamics Eqns

$$\begin{bmatrix} I^{(1)} & -\tilde{I}^{(2)} & I^{(4)} \\ \tilde{I}^{(2)} & I^{(3)} & I^{(5)} \\ I^{(4)t} & I^{(5)t} & I^{(7)} \end{bmatrix} \begin{Bmatrix} \dot{V} \\ \dot{\omega} \\ \dot{\sigma} \end{Bmatrix} + \begin{Bmatrix} I^{(1)} \tilde{\omega} V + \tilde{\omega} (\tilde{\omega} I^{(2)} + I^{(4)} \sigma) \\ I^{(2)} \tilde{\omega} V + \tilde{\omega} I^{(3)} \omega + \sum_j^n I_j^{(8)t} \sigma_j \omega \\ I^{(4)t} \tilde{\omega} V + W \end{Bmatrix} = \begin{Bmatrix} R_1 \\ R_2 \\ R_3 \end{Bmatrix} + \begin{Bmatrix} U \\ \tilde{r}_t \\ \phi^t \end{Bmatrix} \dot{m} V_e$$

Dynamical Eqns Involve Variable Mass Modal Integrals, $I^{(j)}$

States are frame origin velocity, angular velocity, efficient modal generalized speeds;

Effects of thrust show up in generalized force and load-dependent geometric stiffness of structure, which affects frequencies.

Computing Variable Mass Modal Integrals in Rocket Dynamics

Approximation:

Modes Not Changing Spatially
with Time: simplifies time-
varying modal integrals via
interpolation

$$m(t) = m_f g(t)$$

$$\begin{aligned} I_j^{(k)} &= \int_0^{m(t)} F^{(k)}(r_0, \phi_j) dm \\ &= g(t) \int_0^{m_f} F^{(k)}(r_0, \phi_j) dm_f \end{aligned}$$

$$g(t) = \left\{ \frac{m_0}{m_f} - \frac{\dot{m}_0 t}{m_f} + \left(\frac{t}{t_f} \right)^2 \left[3 + 2 \frac{\dot{m}_0 t_f}{m_f} - 3 \frac{m_0}{m_f} \right] - \left(\frac{t}{t_f} \right)^3 \left[2 + \frac{\dot{m}_0 t_f}{m_f} - 2 \frac{m_0}{m_f} \right] \right\}$$

Mass at time t modeled by Hermite polynomial in terms of initial mass, mass loss rate, and final mass

Commanded Gimbal Angle, Altitude, Horiz. Disp, Pitch Angle (ICTAM '08)

**Command
gimbal
angle**

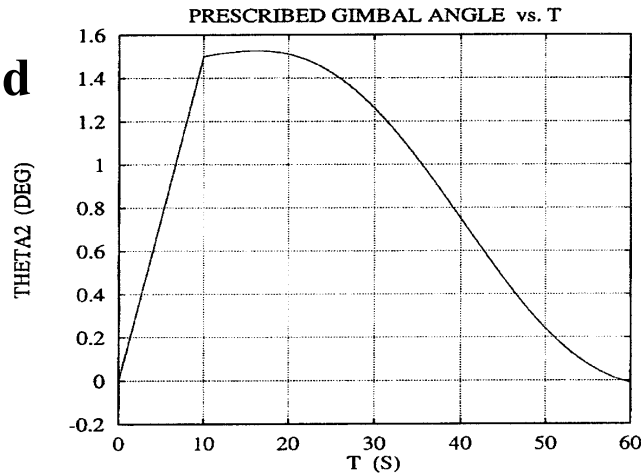


Fig. 2 Prescribed motion time history of the nozzle gimbal angle.

**Rocket
horiz
displ
more for
high flex**

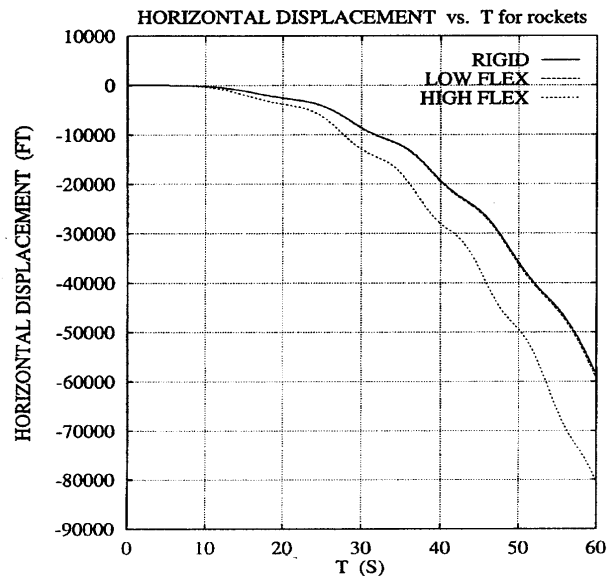


Fig. 4 Horizontal displacement of the rocket vs time, given by three rocket models.

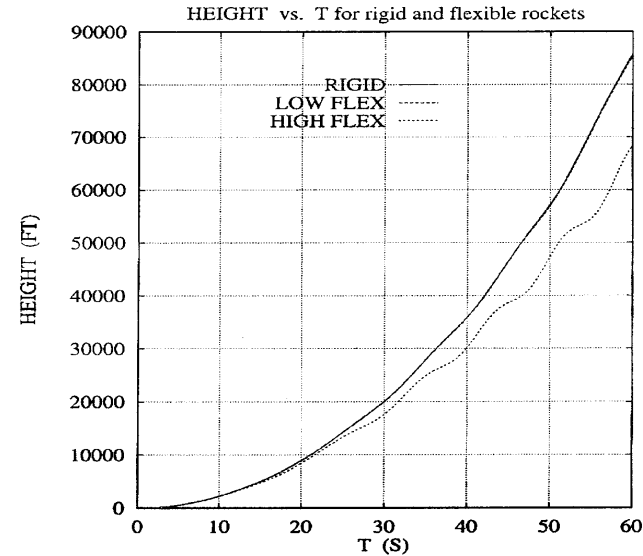


Fig. 3 Height of the rocket from the ground vs time, given by three rocket models.

**Rocket
vertical
disp less
for high flex**

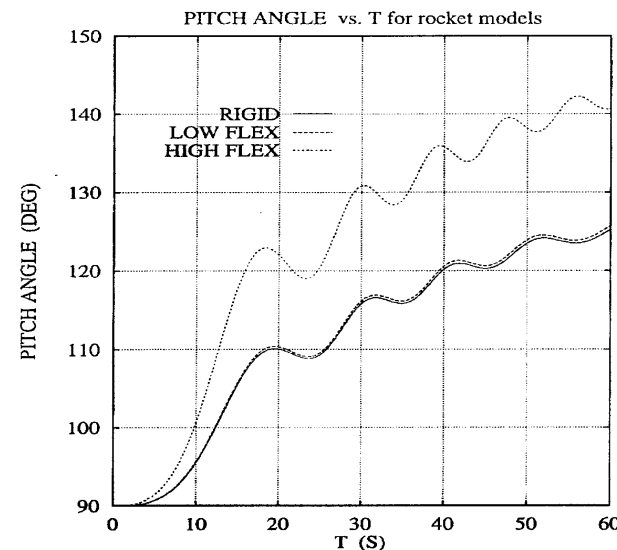


Fig. 5 Pitch angle of the rocket vs time, given by three rocket models.

**Rocket
pitch more
for high
flex**

Tip Defl., First Mode Freqs, Torque for Prescribed Motion (ICTAM '08)

Tip & mid-point (---) defl of high flex rocket

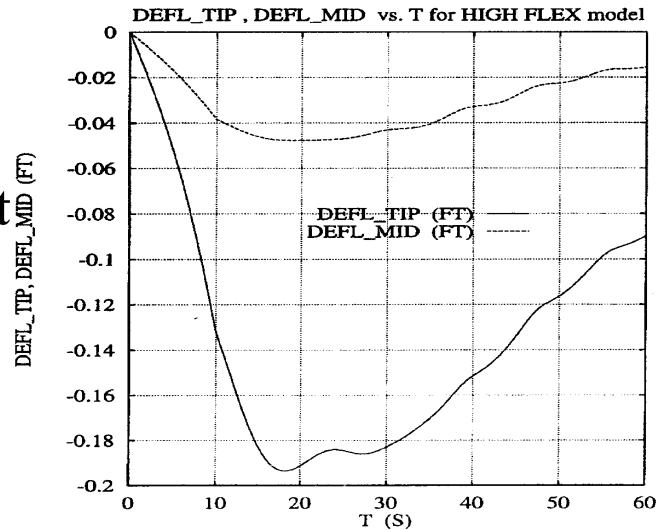


Fig. 6 Tip and midpoint deflection of the high-flexibility rocket model vs time.

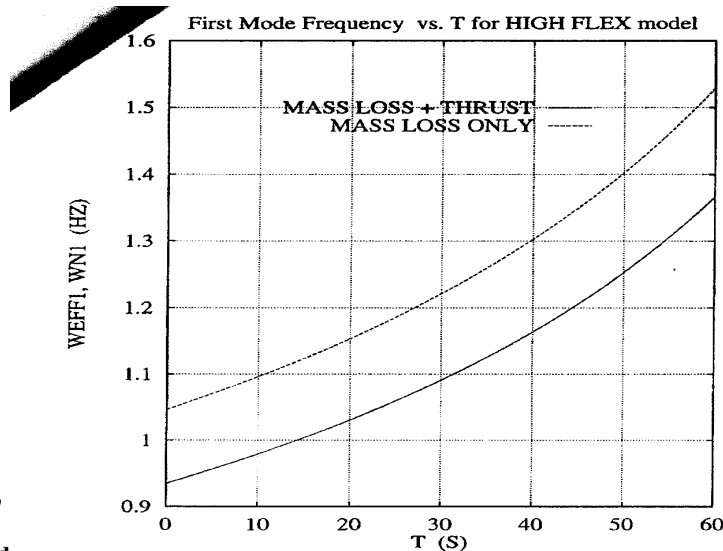


Fig. 7 First mode frequency of high-flexibility rocket model vs time with mass loss only (dotted line) and under the combined action of mass and thrust.

First mode freq for high flex rocket with/wo thrust

First mode freq for low flex rocket w/wo thrust

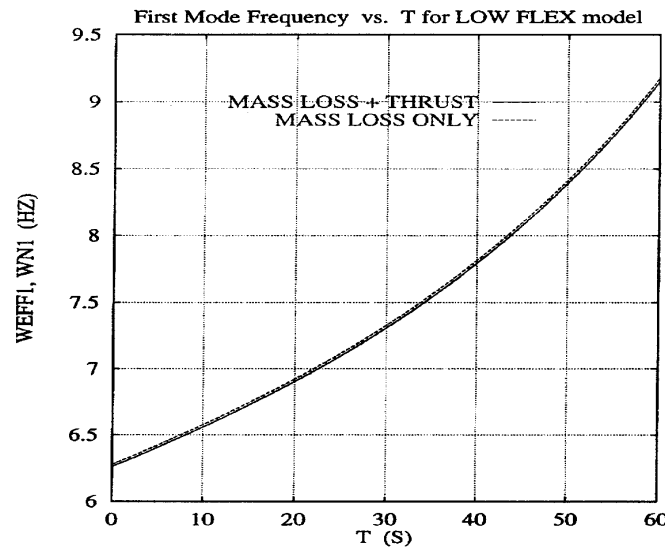


Fig. 8 First mode frequency of low-flexibility rocket model vs time with mass loss only (dotted line) and under the combined action of mass and thrust.

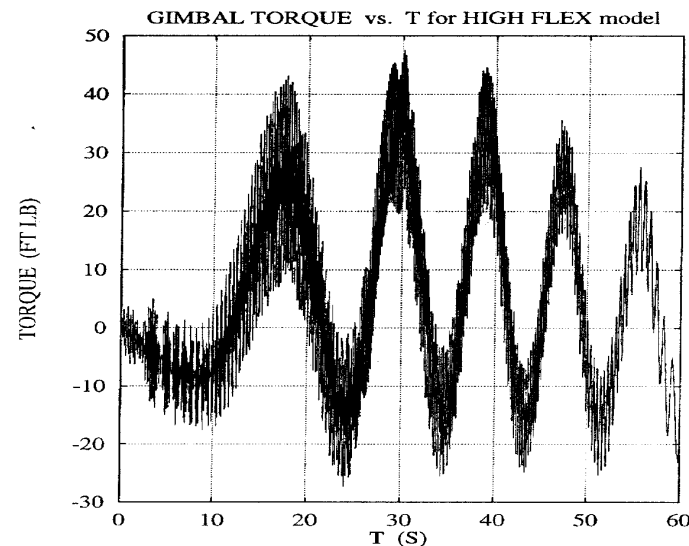


Fig. 9 Gimbal torque in the high-flexibility rocket simulation with specified gimbal motion vs time.

Required gimbal torque for gimbal command angle (high flex case)

CONCLUSION: High-Fidelity, Time-Efficient Modeling of Large Overall Motion of Flexible Multibody Systems

- 1. Computational efficiency increases with i) Block-diagonal recursive Kane formulation, ii) Choosing generalized speeds to simplify dynamical eqns, iii) Representative modal reduction.**
- 2. Geometric stiffness for 12 inertia loads corrects unavoidable error of premature linearization in using vibration modes.**
- 3. Large deflection treated by $O(n)$ formulation with spring-connected rigid multibody models, producing as high-fidelity results as nonlinear FEM, & being more time-efficient.**
- 4. Variable- n $O(n)$ method models deployment / retrieval of beams and cables with fidelity and efficiency.**
- 5. For systems with closed structural loops the recursive method, employed by cutting loops & solving constraint forces, is efficient.**
- 6. Kane's eqns for variable mass flexible bodies, modal integrals via Hermite interpolation, with freqs modified by thrust, are given.**

UPCOMING BOOK: FLEXIBLE MULTIBODY DYNAMICS, BANERJEE: WILEY PUBLICATIONS, N.Y., 2016

